Available online at www.sciencedirect.com
ScienceDirect
Bioorganic & Medicinal Chemistry 16 (2008) 2011–2033
Bioorganic & Medicinal Chemistry

Phenylalanine-containing hydroxamic acids as selective inhibitors of class IIb histone deacetylases (HDACs)

Stefan Schäfer,[a] Laura Saunders,[b] Elena Eliseeva,[c] Alfredo Velena,[c] Mira Jung,[c] Andreas Schwienhorst,[d] Anja Strasser,[e] Achim Dickmanns,[e] Ralf Ficner,[e] Sonja Schlimme,[f] Wolfgang Sippl,[f] Eric Verdin[b] and Manfred Jung[a,*]

[a]*Institute of Pharmaceutical Sciences, University of Freiburg, Albertstr. 25, 79104 Freiburg, Germany*
[b]*Gladstone Institute of Virology and Immunology, University of California, San Francisco, 1650 Owens Street, San Francisco, CA 94158, USA*
[c]*Department of Radiation Medicine, Lombardi Cancer Center, Georgetown University Medical Center, Washington, DC, USA*
[d]*Department of Molecular Genetics and Preparative Molecular Biology, Institute for Microbiology and Genetics, University of Goettingen, Grisebachstr. 8, 37077 Goettingen, Germany*
[e]*Department of Molecular Structural Biology, Institute for Microbiology and Genetics, University of Goettingen, Grisebachstr. 8, 37077 Goettingen, Germany*
[f]*Institute of Pharmacy, Martin-Luther University Halle-Wittenberg, Wolfgang-Langenbeckstr. 4, 06120 Halle (Saale), Germany*

Received 14 August 2007; revised 22 October 2007; accepted 30 October 2007
Available online 4 November 2007

Abstract—We synthesized biarylalanine-containing hydroxamic acids and tested them on immunoprecipitated HDAC1 and HDAC6 and show a subtype selectivity for HDAC6 that was confirmed in cells by Western blot (tubulin vs histones). We obtained an X-ray structure with a HDAC6-selective inhibitor with the bacterial deacetylase HDAH. Docking studies were carried out using HDAC1 and HDAC6 protein models. Antiproliferative activity was shown on cancer cells for selected compounds.

1. Introduction

Enzymes catalyzing the posttranslational modifications of chromatin, for example, histone acetyltransferases (HATs) and histone deacetylases (HDACs), have emerged as new targets for cancer therapy. Since the inhibition of HDACs leads to growth arrest, differentiation or apoptosis of tumour cell lines, clinical studies of HDAC inhibitors for the therapy of cancer are under way. The reversible acetylation and deacetylation of histones and non-histone proteins play important roles in the regulation of chromatin structure and gene expression. Inhibiting the deacetylation of non-histone proteins may be an important contributor to the anticancer activity of HDAC inhibitors.[1,2]

HDACs are divided into three structural classes depending on their homology to yeast proteins. Class I includes four subtypes (HDAC1, 2, 3 and 8) and shows homology to the yeast protein rpd3. Class II consists of six subtypes and is subdivided into two classes, class IIa with subtypes HDAC4, 5, 7 and 9 and class IIb with subtypes HDAC6 and 10. HDAC11 is referred to as class IV. The enzymatic activity of class I and II HDACs occurs in a Zn^{2+}-dependent mechanism. In contrast, the class III HDAC enzymes, also called sirtuins, operate by a NAD^{+}-dependent mechanism. There are seven subtypes in humans (SIRT1-7) which show homology to the yeast protein Sir2.[3]

A wide range of chemical structures including hydroxamic acids, benzamides, electrophilic ketones, thiols and mercaptoamides as well as small fatty acids showing inhibitory potential for Zn^{2+}-dependent HDACs (class I and II) have been developed in the last 10 years.[2,4–6] Our detailed structure–activity relationships led to the

Keywords: Histone deacetylase (HDAC); Class I and II HDAC inhibitor; Hydroxamic acid; Subtype selectivity; Gold docking.
* Corresponding author. Tel.: +49 0761 203 4896; fax: +49 0761 203 6321; e-mail: manfred.jung@pharmazie.uni-freiburg.de

0968-0896/$ - see front matter © 2007 Elsevier Ltd. All rights reserved.
doi:10.1016/j.bmc.2007.10.092

development of various HDAC inhibitors including the potent antiproliferative agent SW55 (**3**).[7,8]

Limited information is available on the structural requirements for HDAC subtype selective inhibition, and especially on the biological significance of subtype selective HDAC inhibitors. Several class I selective inhibitors are available,[9–13] especially for HDAC1, but only a few for specific class II enzymes (HDAC4 or 6).[14,15] Tubacin was reported to be selective for tubulin acetylation[16] but inhibits other subtypes in vitro as well.[17] We set out to obtain structure–activity relationships (SAR) on biarylalanines **4** as analogues of **3**, esp. with regard to subtype selectivity (see Fig. 1). Specifically, we investigated the influence of the spacer length as well as that of the second aryl ring. To elucidate the probable binding mode of the most active inhibitors docking studies were carried out using generated homology models of HDAC1 and HDAC6. These studies are supported by a new X-ray structure of a HDAC6-selective inhibitor with the bacterial deacetylase HDAH.[18]

HDAC1 and 6 were chosen as representative subtypes and served as sources of enzymatic activity. HDAC6 is interesting to study because it is the only subtype that has been shown to deacetylate tubulin, an important anticancer target, and there is limited availability of selective inhibitors for this subtype. Confirmation of the in vitro selectivities in the cell was achieved by comparing histone and tubulin acetylation via Western blot. Additionally, the antiproliferative properties of selected inhibitors were compared.

2. Results

2.1. Chemistry

The synthesis of the new series of compounds was carried out in a six-step synthesis from *p*-bromophenylalanine methyl ester (**5**) in analogy to previous work from our group[7,8] and is shown in Scheme 1. Compounds **8a**, **9a** and **10a** have been described before, and by using monomethylazelate (**7**) instead of suberoylchloride (**6**) the respective homologues were obtained. **10a** and **10b** were then coupled in a microwave-assisted Suzuki-coupling reaction with arylboronic acids which led to the protected biarylalanine-containing hydroxamates **11a–m**. The biaryls **11** and the bromophenylalanines **10a–b** were then deprotected and the desired inhibitors **4a–o** were obtained.

2.2. Enzyme inhibition

In a first test series the compounds **4a–o** were assayed using purified rat liver extract as a HDAC source and an unselective small molecule substrate in a homogeneous assay (see Section 4) developed in our group. The inhibitors CHAP15,[10] M344[19] and **3**[7] were included for comparisons. All compounds showed inhibitory potency between 270 nM and 5.1 μM (Table 1). Most compounds are active below 1 μM but with the bromo derivatives **4n** and **4o** the potency was increased compared to the lead structure **3** (see Table 1). Among the biaryl analogues the most potent compound is the ter-

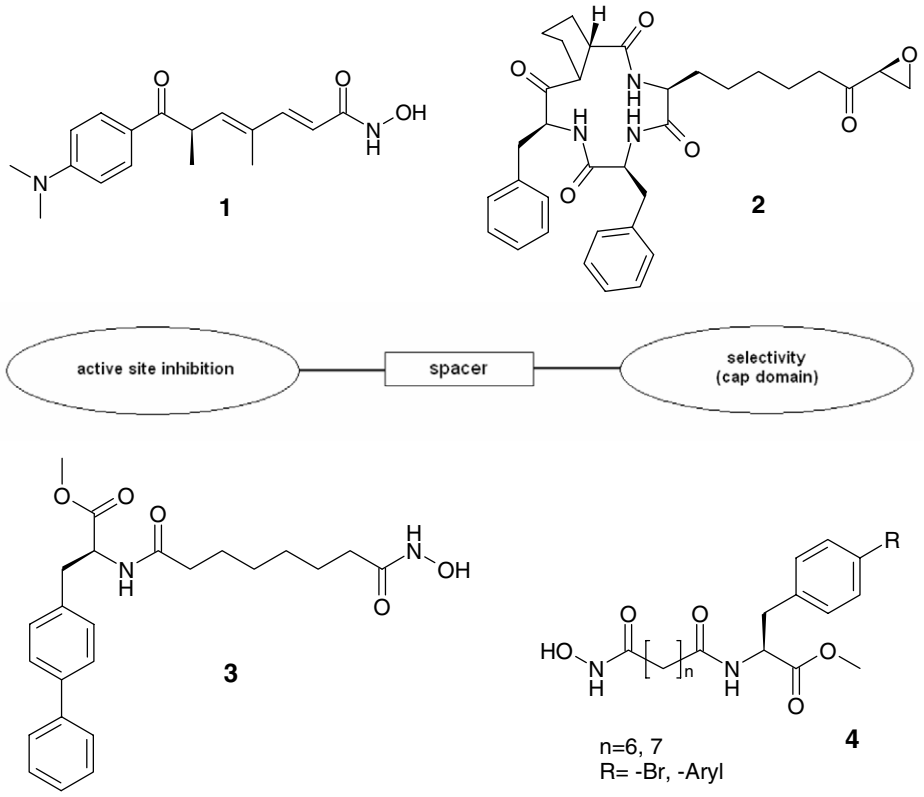

Figure 1. HDAC inhibitors: TSA (**1**), trapoxin (**2**), SW55 (**3**), general structure for new inhibitors **4**.

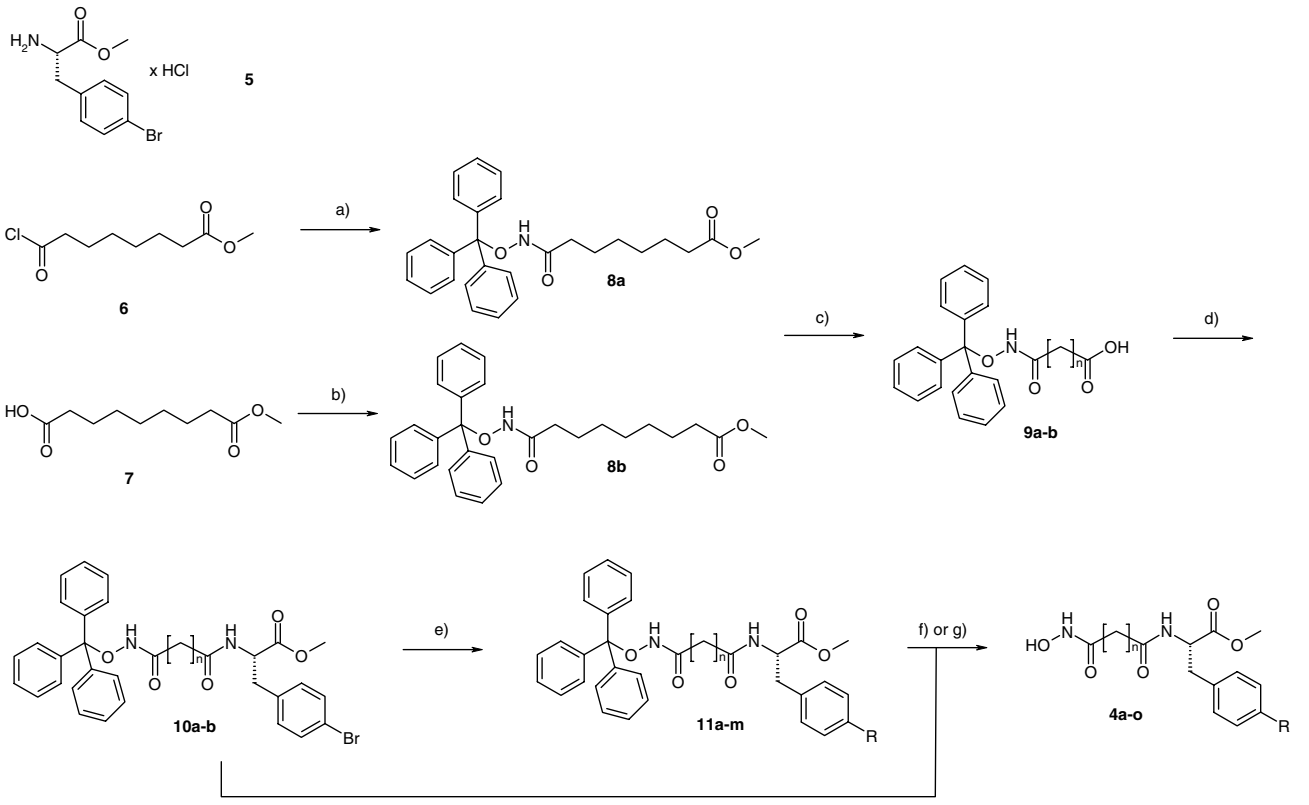

Scheme 1. Reagents and conditions: (a) *O*-tritylhydroxylamine, DIPEA, DCM, 0 °C; (b) *O*-tritylhydroxylamine, IBCF, NMM, THF, −10 °C; (c) LiOH, H_2O_2, THF; (d) **5**, IBCF, NMM, THF, −10 °C; (e) R-B$(OH)_2$, tri-*o*-tolylphosphine, $Pd(OAc)_2$, Na_2CO_3, DME, H_2O, microwave: 5–10 min, 100 W; (f) TFA, TES, 0 °C (**4a**–**j**, **4l**–**o**); (g) TSMTF, TES, 0 °C (**4k**).

Table 1. HDAC-inhibitory activity of **4a**–**o**

Enzyme			$IC_{50} \pm SE$ (μM)				
			Rat liver extract			HDAC1	HDAC6
Compound	*n*=	R=	Subtype selectivity of substrate				
			None	HDAC1	HDAC6	None	None
CHAP15[a]	—	—	0.14 ± 0.01	0.021 ± 0.003	0.23 ± 0.02	0.0004 ± 0.0002	0.04 ± 0.01
M344[a]	—	—	0.07 ± 0.01	0.24 ± 0.04	0.08 ± 0.01	2.96 ± 1.39	0.75 ± 0.09
3	6	–Phenyl	0.50 ± 0.03	0.44 ± 0.13	0.58 ± 0.06	1.22 ± 0.20	1.05 ± 0.18
4a	7	–Phenyl	0.70 ± 0.07	1.68 ± 0.47	6.10 ± 0.42	9.54 ± 1.72	2.33 ± 0.45
4b	6	–2-Thienyl	0.64 ± 0.09	0.57 ± 0.07	0.58 ± 0.03	5.07 ± 1.12	9.99 ± 1.83
4c	7	–2-Thienyl	1.16 ± 0.12	2.55 ± 0.47	0.84 ± 0.08	16.75 ± 1.42	4.09 ± 1.04
4d	6	–3-Thienyl	0.81 ± 0.15	0.59 ± 0.10	0.50 ± 0.04	3.34 ± 0.37	4.02 ± 2.92
4e	7	–3-Thienyl	0.87 ± 0.06	3.01 ± 0.19	0.81 ± 0.02	19.19 ± 3.98	1.77 ± 0.08
4f	6	–2-Furyl	1.00 ± 0.13	7.53 ± 0.85	6.76 ± 0.41	2.61 ± 1.68	4.49 ± 0.21
4g	7	–2-Furyl	1.00 ± 0.06	2.44 ± 0.23	0.47 ± 0.10	9.76 ± 1.72	2.33 ± 0.42
4h	6	–3-Furyl	0.86 ± 0.08	3.18 ± 0.65	2.25 ± 0.20	6.35 ± 0.64	1.13 ± 0.34
4i	7	–3-Furyl	1.13 ± 0.07	3.03 ± 0.31	0.68 ± 0.04	10.30 ± 0.54	1.05 ± 0.18
4j	6	–Biphenyl	0.66 ± 0.13	0.13 ± 0.01	0.78 ± 0.05	0.96 ± 0.39	0.69 ± 0.21
4k	7	–Biphenyl	0.99 ± 0.26[b]	8.76 ± 1.26[c]	6.76 ± 0.83	38.28 ± 4.48	14.72 ± 2.67
4l	6	–2-Naphthyl	1.07 ± 0.06	0.63 ± 0.04	0.91 ± 0.05	2.98 ± 0.16	1.17 ± 0.13
4m	7	–2-Naphthyl	5.12 ± 0.74	5.19 ± 1.22[d]	3.76 ± 0.59[d]	10.54 ± 0.99	2.85 ± 1.97
4n	6	Br	0.27 ± 0.04	3.19 ± 0.52	4.98 ± 0.27	22.86 ± 7.25	1.69 ± 0.91
4o	7	Br	0.43 ± 0.06	2.11 ± 0.31	0.68 ± 0.06	28.44 ± 1.61	4.67 ± 2.76

[a] Data taken from lit.[21]
[b] Max. inhibition: 55%.
[c] Max. inhibition: 60%.
[d] Values determined using the trypsin assay.

phenyl **4j** with a six-carbon spacer while the 2-naphthyl substituent in **4l**–**m** leads to a decrease in rat liver HDAC inhibition (see Table 1).

All compounds were tested for the inhibition of immunoprecipitated FLAG-HDAC1 and 6. For these enzymes another small molecule substrate[20] was used

which shows higher conversion rates with the isolated subtypes as compared to the rat liver substrate and has no subtype selectivity. Again, for both subtypes the terphenyl **4j** displayed the most potent inhibition and it exceeded the lead structure **3** in its inhibitory activity.

We have previously reported that HDAC-subtype selective substrates can be used in inhibition assays with purified rat liver extracts containing a mixture of HDAC subtypes to get an indication of actual subtype selectivity.[21] Therefore, we used our new set of inhibitors to test the predictive power of these substrates on a larger set of compounds. We compared the IC_{50}-values obtained with the subtype selective substrates and a mixture of subtypes (rat liver extract) with the respective ratios obtained with the subtypes and an unselective substrate (see Table 2). A minimum factor of three was arbitrarily chosen to state selectivity.

None of the inhibitors showed a pronounced selectivity for HDAC1 although in two cases (**4a** and **4j**) such a selectivity was predicted. On the other hand, nine compounds showed selectivity for HDAC6 of which five cases were predicted. All biaryls predicted to be HDAC6 selective indeed showed that selectivity but the bromophenylalanine that was shown to be the most selective compound (**4n**) was missed. Altogether, the inhibitors **4e**, **4h**, **4i**, **4n** and **4o** showed pronounced (more than fivefold) selectivity for HDAC6. In compounds with the same biaryl group the inhibitors with a spacer length of 7 methylene groups displayed a higher selectivity for HDAC6 than the congeners with the shorter spacer. The selectivity is the highest for heterobiaryls with the connecting bond in the 3′-position (**4e** and **4i**). The trend regarding the dependence of the selectivity on the spacer length is reversed in the bromo substituted compounds where the suberoyl analogue **4n** is more selective than the azelaic acid derivative **4o**. The highest affinity to one of the subtypes is seen with the terphenylalanine **4j** with the short spacer (700 nM for HDAC6).

Table 2. Selectivity indices

Compound	Substrates HDAC1/HDAC6	Subtypes HDAC1/HDAC6
CHAP15[a]	0.09	0.01
M344[a]	3.00	3.95
3	0.76	1.16
4a	0.28	4.09
4b	0.98	0.51
4c	3.04	4.10
4d	1.18	0.83
4e	3.72	10.84
4f	1.11	0.58
4g	5.19	4.19
4h	1.41	5.62
4i	4.46	9.81
4j	0.17	1.39
4k	1.30	2.60
4l	0.69	2.55
4m	1.38	3.70
4n	0.64	13.53
4o	3.10	6.09

The predicted selectivities are obtained by dividing the IC_{50} values obtained with rat liver HDAC and the subtype selective substrates (HDAC1/HDAC6), respectively, the measured selectivities by dividing the IC_{50} values obtained with immunoprecipitated subtypes and a non-selective substrate (HDAC1/HDAC6).

[a] Data taken from lit.[21]

For confirmation of the observed selectivity we analyzed the extent of histone vs. tubulin acetylation for selected inhibitors **4d**, **4e** and **4n**. HDAC1 activity is mostly correlated to histone deacetylation, whereas HDAC6 activity should be responsible for a preference in tubulin deacetylation. We were able to demonstrate a hyperacetylation in the low micromolar range with regard to tubulin for the HDAC6 selective inhibitors **4e** and **4n**, whereas the unselective **4d** as well as the control TSA (**1**) show a hyperacetylation of both tubulin and histones (Fig. 2).

2.3. Analysis of the HDAC binding sites and inhibitor binding modes

The X-ray crystallographic analysis of bacterial histone deacetylase-like proteins (HDLP and FB188 HDAH)[18,22–24] as well as HDAC7 and HDAC8[18,25] complexes with **1** (see Fig. 1) or suberoylanilide hydroxamic acid (SAHA) has shown that the HDAC catalytic domain consists of a narrow tube-like pocket spanning a length equivalent to a straight chain of four to six carbons. Two conserved aromatic residues of HDAC enzymes (Phe152 and Phe208 in FB188 HDAH, Phe152 and Phe208 in HDAC8) located in the tube-like pocket fix the position of the flexible alkyl spacer of the inhibitors. The catalytic zinc ion buried near the bottom of the active site is coordinated by His and Asp residues and the hydroxamic acid function of the inhibitors. A similar architecture and interaction pattern is assumed for the related HDAC1 and HDAC6 enzymes.

Only for HDAC1 a few homology models have already been published and used to explain the interaction of TSA or SAHA analogues.[26–28] However, they all were based on the crystal structure of the bacterial homologue HDLP which shows only moderate sequence identity to the human HDACs. In order to better consider the specific architecture of human HDACs we initiated a homology modelling approach using the very recently solved X-ray structures of human HDAC8, HDAC7 and the bacterial FB188 HDAH.[18,22,23,25] HDAC6 is unique among deacetylases in having two HDAC catalytic domains (HDAC6 CD I and HDCA6 CD II) sharing 46% sequence identity and 60% similarity, respectively. The presence of two catalytic domains within HDAC6 makes it difficult to understand how these active sites contribute to the biochemistry and cellular physiology. There are conflicting results and interpretations in the HDAC6 literature. Work from Zhang et al.[29] suggested that both domains are active as histone deacetylases. In a more detailed study using natural and synthetic substrates Zou et al. recently showed that the second catalytic site is the major functional domain of HDAC6.[30] They analyzed highly purified human recombinant

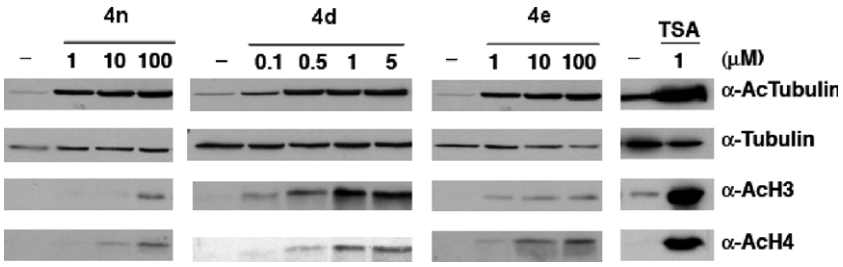

Figure 2. Western blots of HCT116 cells incubated with **4d**, **4e**, **4n** and TSA (**1**).

HDAC6 and demonstrated that the inhibition of HDAC6 by inhibitors can be solely attributed to the interaction with the second binding domain. To address the question whether both catalytic domains are potential binding sites for the hydroxamic acid derivatives, protein models for both catalytic domains of HDAC6 (CD I and II) were generated and analyzed. A detailed description of the protein modelling together with the sequence alignment is given in Section 4 and in the Supporting Material.

The derived HDAC1, HDAC6 CD I and HDAC6 CD II protein models show high structural similarity in the catalytic regions, whereas larger deviations can be observed at the entrance region of the binding pocket (Fig. 3a–d). In Figure 3a–d the HDAC1, HDAC6 CD I and HDAC6 CD II models are superimposed with the template structures used for the homology modelling, HDAC8 and HDAC7, respectively. Especially the loop regions forming the entrance of the binding cavity are dissimilar in the different HDAC structures. On the other hand, the

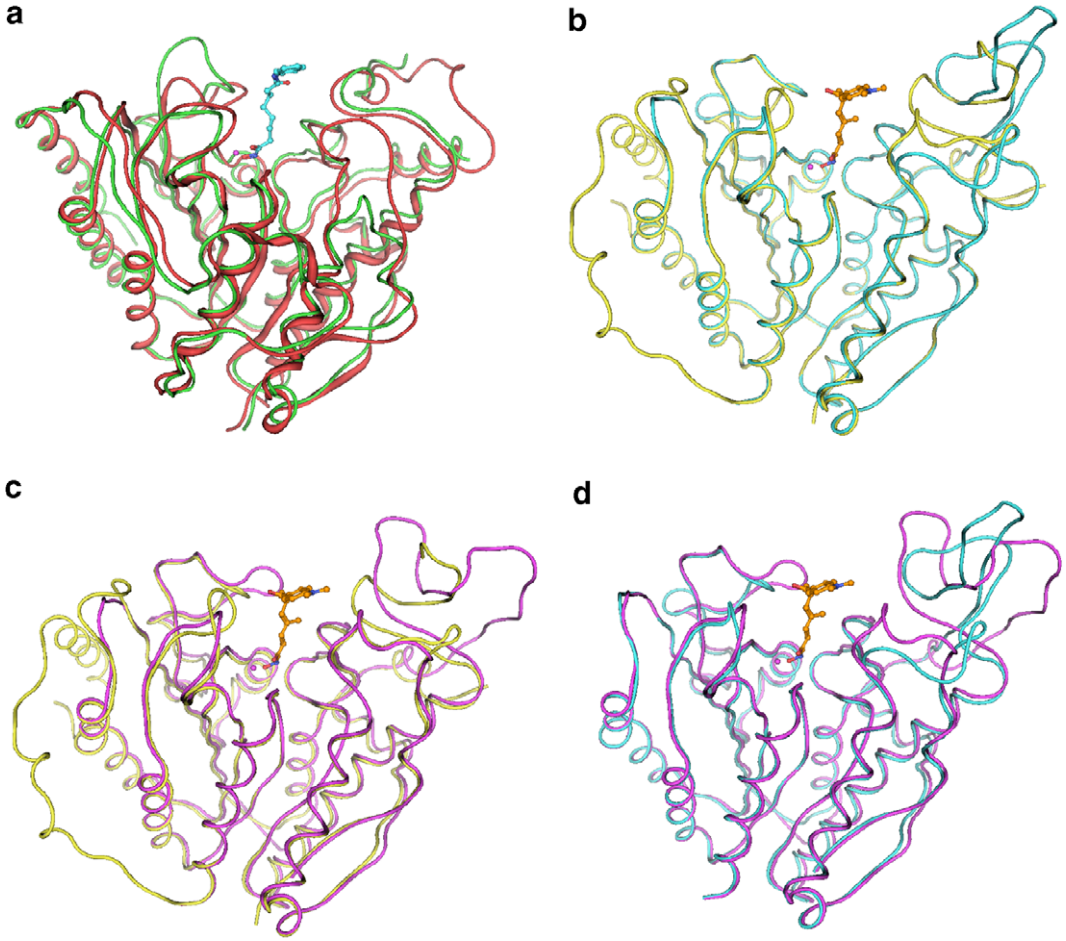

Figure 3. (a) Superimposition of the HDAC8 X-ray structure (green ribbon) with the co-crystallized inhibitor TSA (**1**) (cyan) and the HDAC1 homology model (red tube) (RMSD backbone atoms 1.8 Å). The zinc ion is coloured magenta. (b) Superimposition of the HDAC7 X-ray structure (yellow ribbon) with the co-crystallized inhibitor TSA (**1**) (orange) and the HDAC6 CD I model (cyan ribbon). (RMSD backbone atoms 1.5 Å.) The zinc ion is coloured magenta. (c) Superimposition of the HDAC7 X-ray structure (yellow ribbon) with the co-crystallized inhibitor TSA (**1**)and the HDAC6 CD II model (magenta ribbon). (RMSD backbone atoms 2.9 Å). The zinc ion is coloured magenta. (d) Superimposition of the HDAC6 CD I model (cyan ribbon) and the HDAC6 CD II model (magenta ribbon). (RMSD backbone atoms 2.2 Å.) The zinc ion is coloured magenta.

zinc binding site (Fig. 4a and b) shows high similarity between the different HDAC structures.

The generated HDAC1 and HDAC6 protein models as well as FB188 HDAH were subsequently used for ligand docking studies. In advance of docking the novel inhibitors into the HDAC1 and HDAC6 homology models, we first tested whether the docking program GOLD[31] is able to reproduce the experimentally observed HDAC inhibitor binding modes. For this purpose we took the

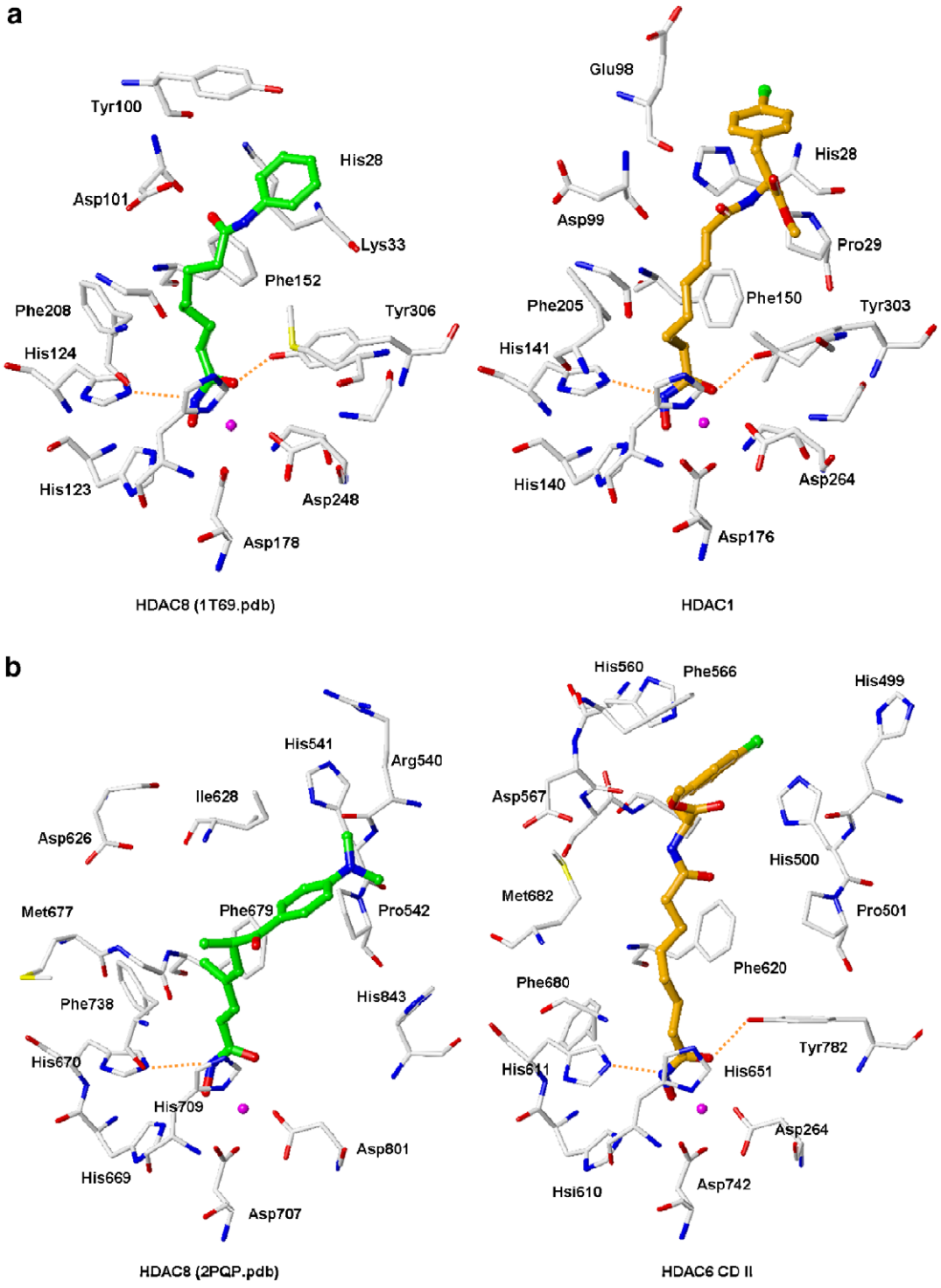

Figure 4. (a) Comparison of the HDAC8 X-ray structure (1T69.pdb, left site) with the co-crystallized inhibitor SAHA (coloured green) and the HDAC1 homology model (right site) with the docked inhibitor **4n** (coloured orange). Only the binding pocket residues are shown. Hydrogen bonds are displayed as dashed line. (b) Comparison of the HDAC7 X-ray structure (2PQP.pdb, left site) with the co-crystallized inhibitor TSA (**1**) and the HDAC6 CD I model (right site) with the docked inhibitor **4n** (coloured orange). Only the binding pocket residues are shown. Hydrogen bonds are displayed as dashed line.

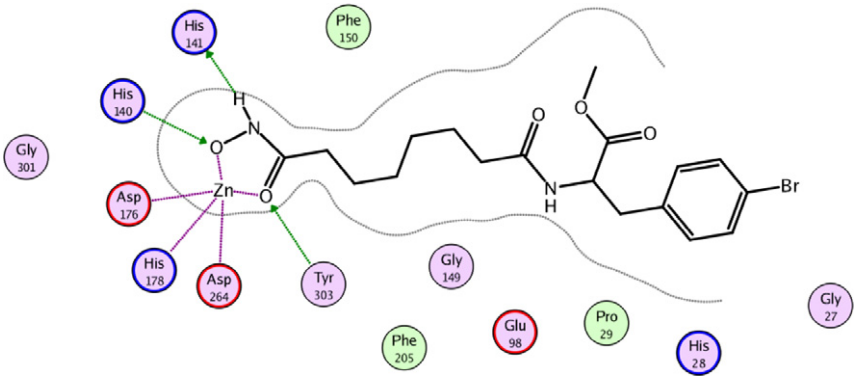

Figure 5. Schematic representation of the interaction between **4n** and HDAC1. Hydrogen bonds are displayed as green arrows, whereas the zinc coordination is indicated by magenta dashed lines.

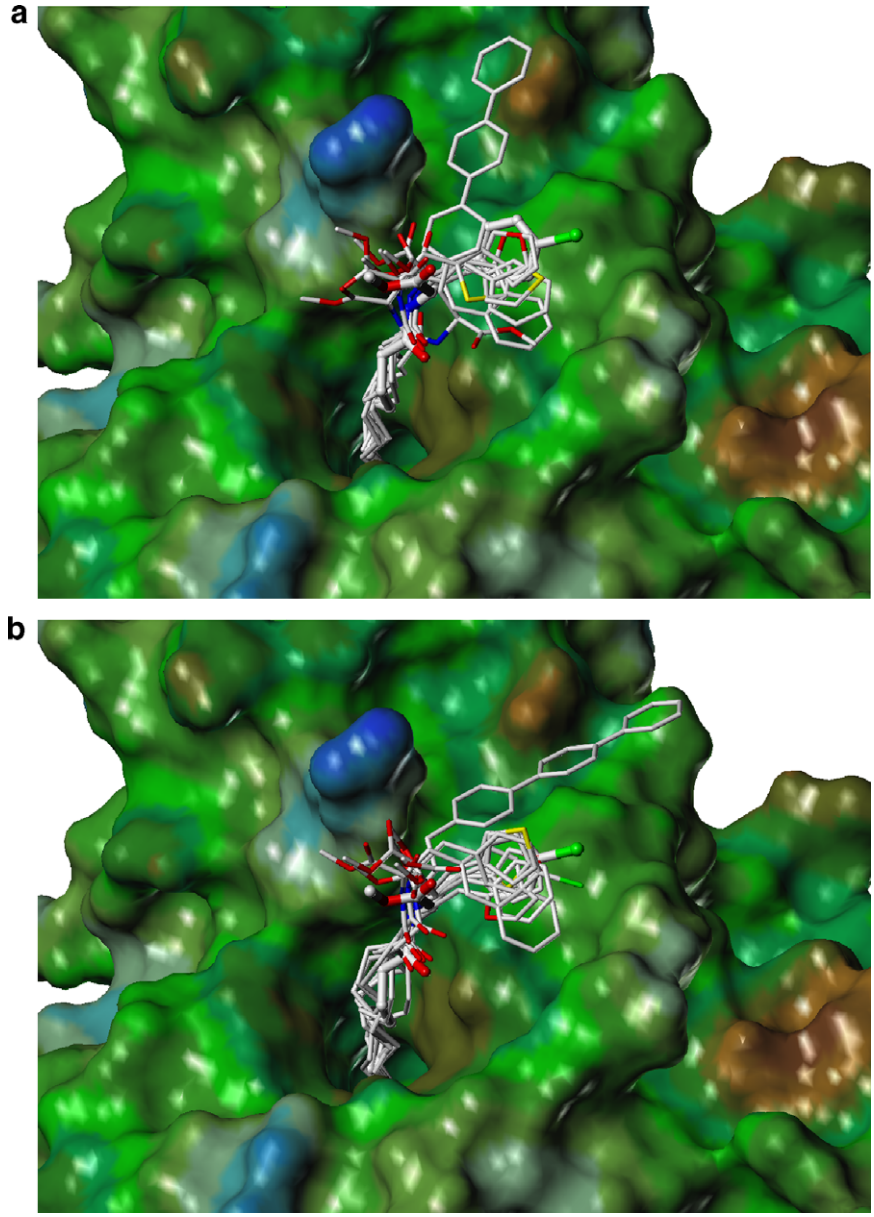

Figure 6. (a) GOLD docking solutions for HDAC1 and inhibitors with a C6-alkyl chain spacer. **4n** is displayed for comparison in ball-and-stick mode. The surface of the HDAC1 binding pocket is coloured according the hydrophilicity (brown = hydrophobic, blue = hydrophilic). (b) GOLD docking solutions for HDAC1 and inhibitors with a C7-alkyl chain spacer. **4n** is displayed for comparison in ball-and-stick mode. The surface of the HDAC1 binding pocket is coloured according the hydrophilicity (brown = hydrophobic, blue = hydrophilic).

published X-ray crystallographic structures of HDACs and FB188 HDAH from the Protein Database[32] as well as the novel solved X-ray structure of FB188 HDAH in complex with **4n** (see below). In case of the X-ray structures of FB188 HDAH complexes with SAHA (pdb code 1ZZ1) and CypX (pdb code 1ZZ3) RMSD values between the best docking solution and the crystal structure were found to be below 1.5 Å (for details, see Supporting Material, Figs. A and B). Additionally, the two observed different conformations of **4n** in the FB188 HDAH crystal structure could be reproduced by GOLD (RMSD values below 1.5 Å, Figs. C and D, Supporting Material).

Next, the bromophenylalanine-containing hydroxamic acid **4n** was docked into the HDAC1 homology model (Figs. 4a and 5). The docking of **4n** as well as the other developed inhibitors into HDAC1 showed that the hydroxamic acid and the alkyl chain interact in a similar way at the binding pocket. The hydroxamic acid function of the inhibitors is located in a polar pocket formed by several residues capable of forming hydrogen bonds (His140, His141 and Tyr303), whereas Phe150 and Phe205 sandwich the hydrophobic alkyl chain of the inhibitor. Van der Waals interactions are also of great importance in the inhibitor-HDAC recognition process, especially for the accommodation of the cap group. The cap group of **4n** interacts with several aromatic and hydrophobic residues at the entrance of the binding pocket (His28, Pro29 and Pro101).

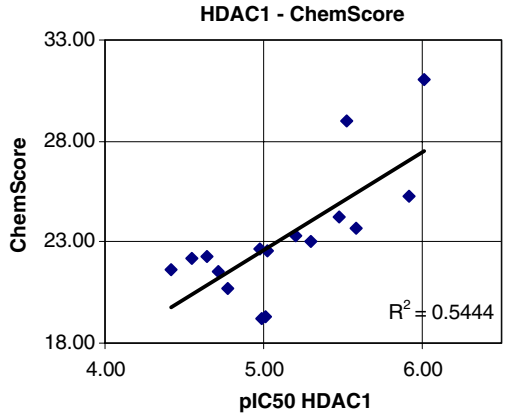

Figure 7. Correlation between obtained ChemScore values and pIC_{50} data for HDAC1.

Next we docked all other newly synthesized inhibitors into the HDAC1 binding pocket and analyzed the binding mode and the obtained ChemScore values. Similar docking poses observed for **4n** could be obtained for the other inhibitors. In this binding mode the cap group interacts with an open cavity at the entrance of the binding pocket formed by several aromatic and hydrophobic residues (His28, Pro29 and Pro101) (Fig. 6a and b). The analysis of the derived ChemScore values showed that they are in qualitative agreement with the experimentally obtained IC_{50}-values for the recombinant HDAC1. The regression analysis for HDAC pIC_{50} and ChemScore values is shown in Figure 7.

In case of the HDAC6 CD I and CD II homology models the entrance of the binding pocket itself shows several clearly defined cavities and offers additional interaction possibilities for the hydrophobic cap groups of the inhibitors (Fig. 3d). The analysis of the docking solutions obtained for both HDAC6 homology models showed a similar binding pattern for the hydroxamic acid inhibitors. His215, His216, Tyr386 in HDAC6 CD I and His610, His611, Tyr782 in HDAC6 CD II form hydrogen bonds to the hydroxamic acid function. Phe283 and Tyr225 in HDAC6 CD I, as well as Phe620 and Phe680 in HDAC6 CD II, sandwich the alkyl chain linker between their hydrophobic portions (Figs. 4b and 8). Larger deviations were observed in the interaction of the bulky cap groups. The HDAC6 CD II model shows a clearly defined hydrophobic binding cavity formed by several aromatic and hydrophobic residues (His499, His560, Phe566, Ile569). For all docked inhibitors the top-ranked pose (based on the

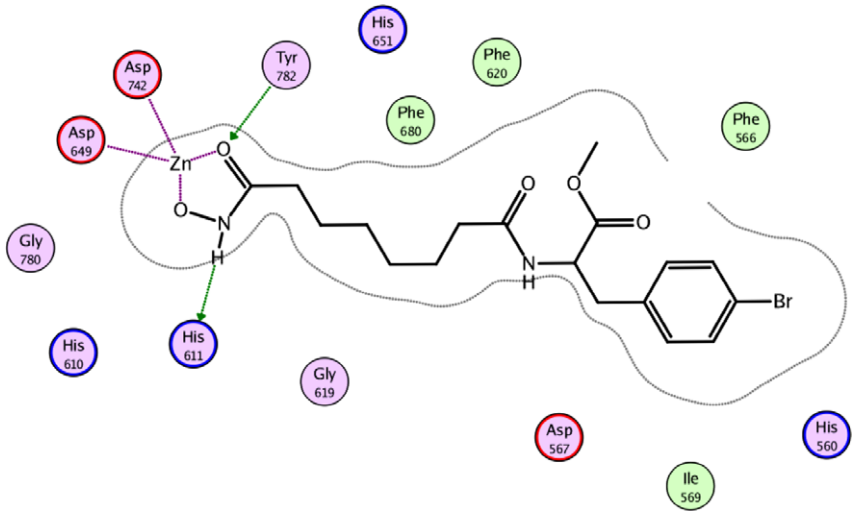

Figure 8. Schematic representation of the interaction between **4n** and HDAC6 CD II. Hydrogen bonds are displayed as green arrows, whereas the zinc coordination is indicated by magenta dashed lines.

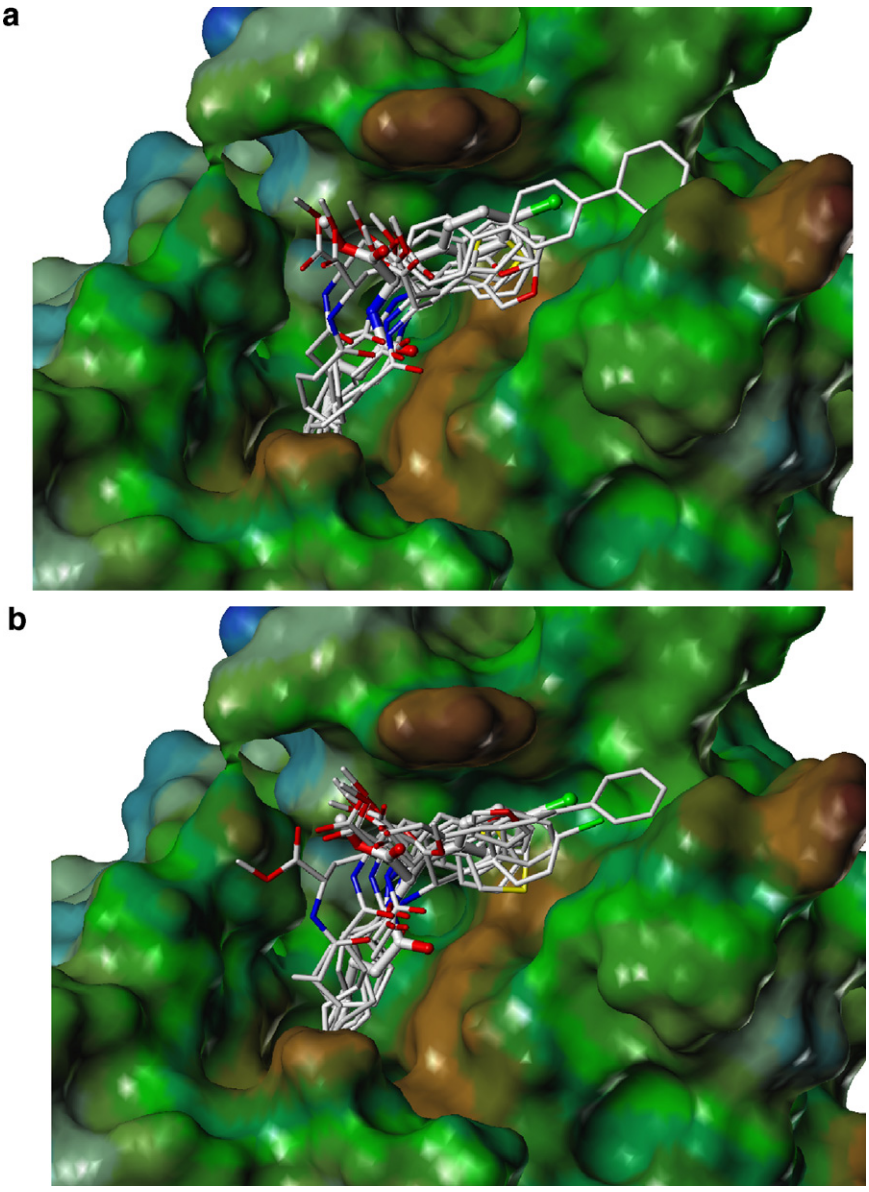

Figure 9. (a) GOLD docking solutions for HDAC6 inhibitors with a C6-alkyl chain spacer. **4n** is displayed for comparison in ball-and-stick mode. The surface of the HDAC6 binding pocket is coloured according the hydrophilicity (brown = hydrophobic, blue = hydrophilic). (b) GOLD docking solutions for HDAC6 inhibitors with a C7-alkyl chain spacer. **4n** is displayed for comparison in ball-and-stick mode. The surface of the HDAC6 binding pocket is coloured according the hydrophilicity (brown = hydrophobic, blue = hydrophilic).

ChemScore) places its hydrophobic cap group in this binding groove (Fig. 9a and b). The highest docking scores were obtained for the C6-spacer compounds containing a bulky cap group (**4j** and **4l**). In general, also for the docking into HDAC6 CD II, the ChemScore values showed a moderate correlation with the experimental biological data (Fig. 10). In case of the HDAC6 CD I model, the docking solutions showed no clear preference for this pocket and several energetically equal docking poses were obtained for the individual compounds (data not shown). In addition, no significant correlation was observed between the ChemScore values and the biological data. Therefore, based on the docking poses and scores, only the HDAC6 CD II model is able to explain the experimentally derived structure–activity relationships. This observation supports the findings of Zou

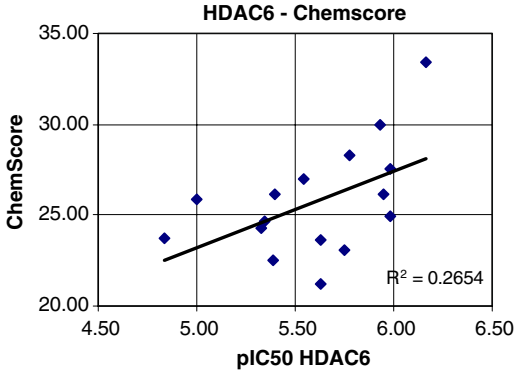

Figure 10. Correlation between obtained ChemScore values and pIC_{50} data for HDAC6.

et al. that the second catalytic domain is the predominant binding site for HDAC6 inhibitors.

The differences in biological activity observed for HDAC1 and HDAC6 were partially clarified by the inspection of the binding mode of the inhibitors and the comparison of the docking scores. The distance between the catalytic centre and the rim of the gorge is shorter in case of HDAC1 compared to HDAC6. Thus, for high HDAC1 activity the six-carbon chain represents the optimal distance between the hydroxamic acid and cap group. This is reflected by the highest docking score for the most active inhibitor **4j** containing a C6-spacer. The biphenyl moiety fits perfectly in the hydrophobic pocket close to Phe566 (Fig. 9a). In case of the C7-spacer compounds, the hydrophobic cap-group is less favourably placed at the solvent-exposed entrance (i.e., more solvent exposed) of the cavity, resulting in decreased biological activity for these compounds. This effect is most dramatic in case of the bulky terphenyl group of compounds **4j** versus **4k**. The HDAC6 binding cavity is longer, resulting in favourable van-der-Waals interactions of the hydrophobic cap group of both series of compounds (C6- and C7-spacer). As a consequence the HDAC6 inhibitory activities of corresponding compounds (C6- and C7-spacer) are very similar. Only in case of the large terphenyl group (**4j** vs **4k**), the cap group of the C7-spacer compound is more solvent exposed, resulting in unfavourable interaction which is reflected by lower docking scores.

In general, the docking poses and scores show a qualitative agreement with the in vitro data obtained for HDAC1 and HDAC6. However, a correlation between the measured selectivity and the structural data was only obtained within the biaryl series.

2.4. Crystal structure

In addition to the modelling studies we were able to obtain a crystal structure of the bacterial FB188 HDAH in complex with a phenylalanine-containing hydroxamic acid which served to verify the predicted inhibitor binding mode. This structure with the bound inhibitor **4n** was determined at 1.9 Å resolution. The inhibitor crystals were in the monoclinic form ($P2_1$). The structure was refined to a free *R*-value of 20.6% with very good stereochemistry (Table 3). The overall structure of FB188 HDAH is essentially the same as described elsewhere.[18] In the inhibitor–HDAH complex the hydroxamate group of **4n** is bound very similar to that of SAHA or CypX.[18] Briefly, the hydroxamate coordinates the zinc ion in the active site through its carbonyl and hydroxyl groups. The hydroxamic acid also hydrogen-bonds with His142 (inner charge-transfer relay) and His143 and the Tyr312 hydroxyl group (see Fig. 11). The two rings of Phe152 and Phe208, which line the active site channel, are in a coplanar orientation and sandwich the spacer region of the inhibitor. In contrast to the electron density of the hydroxamate and long spacer moieties, the electron density of the cap group is rather poorly defined. Similar observations have been reported for other HDAC inhibitors in complexes with FB188 HDAH,[18,24] HDLP[22] or HDAC8[23,33] and have been attributed to a high flexibility of the cap group.

Table 3. X-ray data

Data collection	
Data set	4n
Wavelength (Å)	0.8015
Resolution range[a] (Å)	117.8–1.9 (1.97–1.90)
Space group	$P2_1$
Cell dimensions (Å/°)	$a = 67.7$
	$b = 93.6$
	$c = 121.6$
	$\beta = 104$
Observed reflections	323,438
Redundancy	2.9 (2.4)
Completeness (%)	96.0 (93.8)
R_{sym}[b] (%)	8.5 (38.3)
Average $I/\sigma(I)$	11.2 (2.1)
Mosaicity (°)	0.6
Refinement statistics	
Resolution range[a] (Å)	30–1.9
R_{cryst} (%)/R_{free}[c] (%)	15.6/20.6
FOM	87.9
Coordinate error[d] (Å)	0.090
Bond lengths	0.010
Bond angles	1.345
Chiral	0.088
Ramachandran plot[e]	
Most favourable regions (%)	90.0
Additionally allowed regions (%)	9.6
Generously allowed regions (%)	0.4
Disallowed regions (%)	0
rms deviations from ideality	
Bonds (Å)/angles (°)	0.010/1.344
Average *B* values (Å^2)	16.3
Residues/waters	1474/487

[a] Numbers in parentheses refer to the highest resolution shell.
[b] $R_{sym} = 100 \cdot \sum_h \sum_i |I_i(h) - \langle I(h)\rangle| / \sum_h I(h)$ where $I_i(h)$ is the *i*th measurement of the *h* reflection and $\langle I(h)\rangle$ is the average value of the reflection intensity.
[c] $R_{cryst} = 100 \cdot \sum ||F_o| - |F_c|| / \sum |F_o|$, where F_o and F_c are the structure factor amplitudes from the data and the model, respectively. R_{free} is R_{cryst} with 5% of test set structure factors.
[d] Based on maximum likelihood.
[e] Calculated using PROCHECK.

2.5. Antiproliferative activities

Finally, we tested the effect of the observed selectivities on cytotoxicity in MCF7 breast cancer cells. This screening revealed a correlation between HDAC6-selectivity and a diminished cytotoxicity on the cells. Compounds **4e** and **4n** that presented the highest HDAC6-selectivity showed the least cytotoxicity in this test series (Table 4) but the selective **4h** was among the more active compounds on MCF-7 cells. To verify this correlation, we chose four selective (**4a**, **4e**, **4i** and **4n**) inhibitors as well as one unselective (**4b**) compound and tested them on a panel of different cell lines (Table 5). **4b** is the most toxic compound on all cell lines, whereas the selective compounds again show reduced antiproliferative properties. The Jurkat leukaemia cell line is generally the most sensitive one towards all HDAC inhibitors (Table 5).

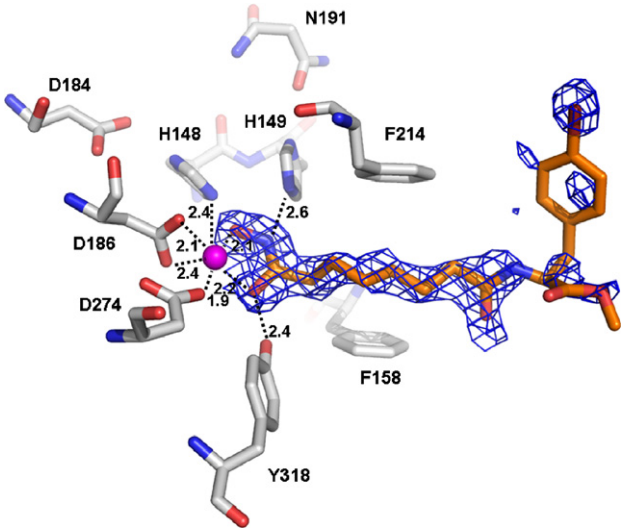

Figure 11. The active site residues of FB188 HDAH with bound inhibitor 4n. Shown are the inhibitor **4n** (C-atoms depicted as orange sticks) and the amino acids of HDAH in close vicinity of the inhibitor (C-atoms in light grey sticks), the bound zinc-ion (purple sphere) and the amino acids proposed to take part in the charge transfer relay systems (Asp184-His148 and Asn191-His149). The electron density map is a $2|F_o - F_c|$ map contoured at 1.0σ. The distance between the two phenylalanines (Phe158 and Phe214) sandwiching the inhibitor is approximately 7.4 Å.

Table 4. Cytotoxicity measurements by cell proliferation assay (MCF-7 cell line)

Compound	IC_{50} (μM)
3	5.0
4a	21.0
4b	4.0
4c	4.0
4d	1.5
4e	17.0
4f	1.5
4g	18.0
4h	1.5
4i	32.0
4j	0.8
4k	3.8
4l	1.9
4m	4.0
4n	22.0
4o	0.9

Table 5. Cytotoxicity measurements by cell proliferation assay on selected compounds

Cell line	IC_{50} (μM)				
	4a	**4b**	**4e**	**4i**	**4n**
SQ20B (adenocarcinoma)	33.0	6.0	37.0	35.0	25.0
HeLa (cervix cancer)	7.0	3.0	10.0	21.0	15.0
Jurkat (leukaemia)	2.7	0.4	2.8	4.0	3.0
MCF10A (non-malignant breast epithelial cell)	42.0	8.0	32.0	44.0	>50
PC3 (prostate cancer)	9.9	1.8	10.0	10.0	>50
MCF7 (breast cancer)	21.0	4.0	17.0	32.0	22.0

Table 6. Elemental analyses of **4a–o**

Compound	Calculated			Found		
	% C	% H	% N	% C	% H	% N
4a	68.16	7.32	6.36	68.21	7.40	6.11
4b	61.09	6.52	6.48	61.07	6.58	6.31
4c	61.86	6.77	6.27	61.87	6.83	6.13
4d	61.09	6.52	6.48	61.06	6.67	6.29
4e	61.86	6.77	6.27	61.78	6.83	6.00
4f	63.45	6.78	6.73	63.10	7.01	6.48
4g	64.17	7.02	6.51	64.18	7.19	6.37
4h	63.45	6.78	6.73	63.16	7.05	6.64
4i	64.17	7.02	6.51	63.79	6.99	6.43
4j	71.69	6.82	5.57	71.02	6.98	6.42
4k	72.07	7.02	5.42	72.07	7.03	5.30
4l	70.57	6.77	5.88	70.56	6.85	5.71
4m	71.00	6.99	5.71	70.92	7.11	5.62
4n	50.36	5.87	6.53	50.59	6.09	6.44
4o	51.48	6.14	6.32	51.63	6.18	6.14

3. Conclusion

Structure–activity studies on biarylalanine inhibitors of HDACs have led to the development of selective HDAC6 inhibitors. We identified structural factors that favour such selectivity (azelaic acid spacer, 3-heteroaryl substituent) but the most selective compound was the synthetic intermediate with a bromophenylalanine structure and a suberic acid spacer. We gained insight into the structural requirements for the binding of inhibitors to HDAC isoenzymes by docking the inhibitors into homology models of HDAC1 and HDAC6. Compounds having a seven-carbon spacer show decreased inhibitory activity for HDAC1 compared to the compounds with a six-carbon spacer. The reason for that is the smaller entrance of the HDAC1 binding channel and the diminished possibilities to bury the hydrophobic cap group. In case of HDAC6 that has a wider entrance of the binding pocket, formed by several non-polar residues, compounds having a longer seven-carbon spacer (e.g., **4e**) are able to interact with the non-polar residues at the entrance of the pocket. This observation is in agreement with the solved X-ray structure of **4n** in complex with FB188 HDAH, where the bromophenyl cap group interacts with the hydrophobic residues at the entrance of the binding pocket. Next to thiol based inhibitors that were published[14] while we were finishing this study, these are the most selective in vitro HDAC6 inhibitors developed so far.

In general, the calculated docking scores are in agreement with the in vitro data obtained for HDAC1 and HDAC6. The most active inhibitor **4j** gave the highest ChemScore values for HDAC1 and HDAC6. However, a quantitative correlation between the measured selectivity and the in vitro data was not obtained. The homology models can interpret the activity of the biarylalanines quite well but were limited in the case of the bromophenylalanines which are quite similar. This could not be foreseen. The variability of the biological data adds to the uncertainty of the prediction in that case. However, we have established these models so they can be further probed and possibly refined with the data

available from the literature and from further compounds from our laboratory. Especially interesting is the fact that those models can contribute to the ongoing conflicting discussion about the relevance of the two catalytic sites in HDAC6. Our data support the reports that CD II is the one that has to be considered for further inhibitor design. So our homology models can be added to the set of tools available for HDAC inhibitor optimization but have to be inspected for their validity on a case to case basis as is necessary with every other model.

The predictive power of subtype selective small molecule substrates was investigated and in this structurally biased series the prediction of HDAC6 activity did not lead to false positives but several false negatives were detected. Thus, if a larger number of presumably HDAC6 selective compounds were available, testing on isolated subtypes could be reduced based on the filtering function of these assays. For selected compounds, the selectivity was confirmed in cancer cells based on the investigation of hyperacetylation of established protein targets. Thus, immunoprecipitated HDACs 1 and 6 may be used as screening tools for compounds with intracellular HDAC subtype selectivity. The new HDAC6 inhibitors exhibit antiproliferative properties on cancer cells with a tendency for reduced cytotoxicity. Given the strong synergistic effects observed for a tubulin selective HDAC inhibitor with the proteasome inhibitor bortezomib,[34] our new compounds and further analogues may be useful agents for combination chemotherapy with reduced systemic toxicity.

4. Experimental

4.1. General

Melting points are uncorrected and were determined by using the melting point apparatus SMP2 (Stuart Scientific). Elemental analyses were performed on a Vario EL elemental analyzer (Elementaranalysensysteme GmbH) (Table 6). ESI- and APCI-mass spectra were measured with a LCQ-Advantage mass spectrometer, EI- and CI-mass spectra with a TSQ700 mass spectrometer (Thermoelectron). NMR spectra were recorded on a Unity 300 spectrometer (300 MHz) by Varian and an Avance DRX 400 spectrometer (400 MHz) by Bruker, respectively. Chemical shifts are presented in ppm relative to tetramethylsilane. For the microwave syntheses we used a Discover microwave synthesis system by CEM. The rat liver HDAC was purified with an Äkta prime chromatography system by Amersham Biosciences. The fluorescent assays were performed on microplate readers by BMG (Fluostar Optima) and Molecular Devices (FlexStation), respectively. M344,[19] **3**[7] and small molecule substrates[20,21,35] were prepared according to the literature.

4.2. Synthesis of inhibitors

4.2.1. General procedures

4.2.1.1. Method A. Preparation of amino acid methyl esters. Anhydrous methanol (10 ml/1 mmol amino acid) was cooled down to −15 °C and 3.5 mmol thionylchloride was added slowly. The amino acid (1 mmol) was then added in portions. The mixture was warmed to room temperature and stirred overnight. The solvent was evaporated and the residue was suspended three times in diethyl ether and evaporated again. The remaining residue was suspended in diethyl ether, filtered, washed with diethyl ether three times and dried in high vacuum.

4.2.1.2. Method B. Amide formation from carboxylic acid chlorides. 1 mmol carboxylic acid chloride was dissolved in anhydrous dichloromethane (1 ml/mmol carboxylic acid chloride) and cooled down to −15 °C. A mixture of 3 mmol *N*-ethyldiisopropylamine (DIPEA) and 1 mmol *O*-tritylhydroxylamine in anhydrous dichloromethane (2 ml/mmol carboxylic acid chloride) was added slowly. The solution was stirred for 4 h at −15 °C and overnight at room temperature. The solvent was evaporated and the residue was dissolved in ethyl acetate. The solution was washed three times in each case with hydrochloric acid (2 M), water, sodium bicarbonate solution (5%) and water. After washing with brine and drying over sodium sulfate the product was crystallized from petroleum ether (80–110 °C). The crystals were collected by filtration and the product was dried in high vacuum.

4.2.1.3. Method C. Amide formation using mixed anhydride. 1 mmol carboxylic acid was dissolved in anhydrous tetrahydrofuran (THF, 20 ml/mmol carboxylic acid). 1 mmol *N*-methylmorpholine (NMM) was added to the solution. The reaction mixture was then cooled down to −15 °C and stirred for 5 min. 1 mmol isobutylchloroformate (IBCF) was added and the mixture was stirred for another ten minutes at −15 °C. Afterwards 1 mmol of the amine and another 2 mmol of NMM were added and the mixture was stirred for 15 min at −15 °C and 2 h at room temperature. Afterwards the mixture was poured into hydrochloric acid (2 M) and extracted three times with ethyl acetate. The organic layers were pooled and washed three times in each case with water, sodium bicarbonate solution (5%) and water. After washing with brine and drying over sodium sulfate the product was crystallized from petroleum ether (80–110 °C). The crystals were collected by filtration and the product was dried in high vacuum.

4.2.1.4. Method D. Ester cleavage. 1 mmol of the ester was dissolved in tetrahydrofuran (THF, 4 ml/mmol ester). 4 mmol of a lithiumhydroxide solution (0.5 M) and 1 ml hydrogen peroxide solution (30%) were added and the solution was stirred overnight. Afterwards the mixture was extracted three times with ethyl acetate. The pH of the aqueous layer was adjusted to three with hydrochloric acid (2 M) and extracted three times with ethyl acetate. The organic layers were pooled and washed three times with water and one time with brine. The solution was dried over sodium sulfate and the product was crystallized from petroleum ether (80–110 °C). The crystals were collected by filtration and the product was dried in high vacuum.

4.2.1.5. Method E. Microwave-assisted Suzuki coupling. All Suzuki-coupling reactions for compounds **11a**–**m** were performed in a dried glass vessel under nitrogen atmosphere. 1 mmol arylbromide, 1.5 mmol boronic acid and 0.1 mmol tri-(*o*-tolyl)-phosphine were dissolved in 14 ml 1,2-dimethoxyethane. 2.4 ml degassed water, 0.05 mmol palladium(II)acetate and 2 mmol sodium carbonate were added and the mixture was heated under reflux in a microwave reactor for 5–10 min with a power of 100 W. The crude product was purified by flash chromatography on silica gel using ethyl acetate and cyclohexane (1:1) as mobile phase. The product was crystallized afterwards from ethyl acetate and petroleum ether (80–110 °C). The crystals were collected by filtration and the product was dried in high vacuum.

4.2.1.6. Method F. Removal of trityl protecting groups with trifluoro acetic acid. The trityl protected precursor was dissolved in dichloromethane. The reaction mixture was then cooled in an ice bath and trifluoro acetic acid (TFA) and triethylsilane (TES) were added alternately dropwise until the yellow colour disappeared. The solvent was evaporated. The residue was dissolved in methanol and evaporated until the smell of acetic acid disappeared. The residue was then dissolved in methanol and the product was crystallized from diethyl ether. The crystals were collected by filtration and the product was dried in high vacuum.

4.2.1.7. Method G. Removal of trityl protecting groups with trimethylsilyl trifluoromethanesulfonate. 1 mmol of the trityl protected precursor was dissolved in dichloromethane (20 ml/mmol). 0.01 mmol trimethylsilyl trifluoromethanesulfonate (TMSTF) and 1.2 mmol triethylsilane (TES) were added and the solution was stirred until the yellow colour disappeared. The solvent was evaporated and the residue was dissolved in a mixture of acetic acid and tetrahydrofuran (1:1). After stirring for 30 minutes, an equal volume of water was added and the mixture was extracted three times with ethyl acetate. The organic layers were combined and extracted three times with water and once with brine. The solvent was dried over sodium carbonate, filtered and evaporated. The residue was again dissolved in methanol and evaporated until the smell of acetic acid disappeared. The crude product was purified by flash chromatography on reversed phase material with acetonitrile and water (1:1) as mobile phase. The product was crystallized from methanol and diethyl ether. The crystals were collected by filtration and the product was dried in high vacuum.

4.2.2. (*S*)-2-Amino-3-(4-bromo-phenyl)-propionic acid methyl ester hydrochloride (5). Compound **5** was synthesized by method **A** from L-bromo-phenylalanine (5 g, 20.1 mmol), 250 ml anhydrous methanol and thionylchloride (5.2 ml, 71.8 mmol); yield: 5.82 g (96%) white powder; melting point: 200 °C; MS (CI(NH_3) pos.) *m*/*z* = 258/260 $[C_{10}H_{12}NO_2Br]^+$, 198/200 $[C_8H_8NBr]^+$; IR (ATR) ν (cm^{-1}) = 1740 ($COOCH_3$), ^1H NMR (400 MHz, CD_3OD) δ = 7.53–7.50 (m, 2H, 3′/5′-*H*), 7.21–7.18 (m, 2H, 4′/6′-*H*), 4.33 (pt, 1H, ^3J = 6.8 Hz, ^3J = 6.8 Hz, NH–C*H*–CO), 3.80 (s, 3H, COOCH_3), 3.24 (dd, 1H, ^2J = 14.4 Hz, ^3J = 6.8 Hz, CH–CH_2–Ar), 3.20 (dd, 1H, ^2J = 14.4 Hz, ^3J = 6.8 Hz, CH–CH_2–Ar); ^{13}C NMR (100 MHz, CD_3OD) δ = 169.98 (*C*OOCH$_3$), 134.44 (1′-*C*), 133.00 (3′/5′-*C*), 132.24 (2′/6′-*C*), 122.64 (4′-*C*), 54.87, 53.65 (COO*C*H$_3$, NH–*C*H–CO), 36.70 (CH–*C*H$_2$–Ar).

4.2.3. 7-Trityloxycarbamoyl-heptanoic acid methyl ester (8a). Compound **8a** was synthesized by method **B** from 7-chlorocarbonyl-heptanoic acid methyl ester (4.8 g, 23.2 mmol), 60 ml anhydrous dichloromethane, DIPEA (12.1 ml, 69.9 mmol) and *O*-tritylhydroxylamine (6.52 g, 23.2 mmol); yield: 8.37 g (81%) white powder; melting point: 90 °C; MS (ESI pos.) *m*/*z* = 468 $[M+Na]^+$, 243 $[C_{19}H_{15}]^+$; IR (ATR) ν (cm^{-1}) = 1736 ($COOCH_3$), 1660 (CO–NH–O–Trt); ^1H NMR (400 MHz, $CDCl_3$) δ = 7.74 (br s, 1H, Trt–O–N*H*–CO), 7.47–7.27 (m, 15H, Ar-*H*), 3.65 (s, 3H, COOCH_3), 2.25 (t, 2H, ^3J = 7.5 Hz, CO–CH_2), 1.90–0.91 (m, 10H, (CH_2)$_5$); ^{13}C NMR (100 MHz, $CDCl_3$) δ = 177.20, 174.26 (*C*O), 141.19, 129.20, 128.30 (Ar-*C*), 93.57 (Ph$_3$-*C*), 51.83 (COO*C*H$_3$), 34.36, 31.47 (CO–*C*H$_2$), 29.11, 25.11, 23.64 (*C*H$_2$).

4.2.4. 8-Trityloxycarbamoyl-octanoic acid methyl ester (8b). Compound **8b** was synthesized by method **C** from non-anedioic acid monomethyl ester (2.5 g, 12.3 mmol), 100 ml anhydrous THF, NMM (4.1 ml, 36.9 mmol), IBCF (1.6 ml, 12.3 mmol) and *O*-tritylhydroxylamine (3.5 g, 12.3 mmol); yield: 4.54 g (80%) white powder; melting point: 101 °C; MS (ESI pos.) *m*/*z* = 482 $[M+Na]^+$, 243 $[C_{19}H_{15}]^+$, 239 $[C_{10}H_{18}NO_4Na]^+$; IR (ATR) ν (cm^{-1}) = 1736 ($COOCH_3$), 1663 (CO–NH–O–Trt); ^1H NMR (400 MHz, $CDCl_3$) δ = 7.72 (br s, 1H, Trt–O–N*H*–CO), 7.46–7.28 (m, 15H, Ar-*H*), 3.66 (s, 3H, COOCH_3), 2.27 (t, 2H, ^3J = 7.5 Hz, CO–CH_2), 1.90–0.99 (m, 12H, (CH_2)$_6$); ^{13}C NMR (100 MHz, $CDCl_3$) δ = 177.07, 174.11 (*C*O), 140.98 128.98, 128.08 (Ar-*C*), 93.57 (Ph$_3$-C) 51.61 (COO*C*H$_3$), 34.21, 31.31 (CO–*C*H$_2$), 29.06, 29.04, 25.03, 23.56 (*C*H$_2$).

4.2.5. 7-Trityloxycarbamoyl-heptanoic acid (9a). Compound **9a** was synthesized by method **D** from **8a** (8.3 g, 18.6 mmol), 50 ml THF, 100 ml lithiumhydroxide solution (0.5 M) and 16 ml hydrogen peroxide solution (30%); yield: 6.4 g (80%) white powder; melting point: 142 °C; MS (ESI pos.) *m*/*z* = 454 $[M+Na]^+$, 243 $[C_{19}H_{15}]^+$; IR (ATR) ν (cm^{-1}) = 1737 (COOH), 1674 (CO–NH–O–Trt); ^1H NMR (400 MHz, $CDCl_3$) δ = 7.46–7.28 (m, 15H, Ar-*H*), 2.25 (t, 2H, ^3J = 7.5 Hz, CO–CH_2), 1.86–0.99 (m, 10H, (CH_2)$_5$); ^{13}C NMR (100 MHz, $CDCl_3$) δ = 178.91, 177.69 (*C*O), 141.18, 129.22, 128.30 (Ar-*C*), 93.64 (Ph$_3$-*C*), 34.20, 31.42 (CO–*C*H$_2$), 29.03, 24.83, 23.63 (*C*H$_2$).

4.2.6. 8-Trityloxycarbamoyl-octanoic acid (7b). Compound **9b** was synthesized by method **D** from **8b** (1.16 g, 2.4 mmol), 50 ml THF, 14 ml lithiumhydroxide solution (0.5 M) and 7 ml hydrogen peroxide solution (30%); yield: 0.8 g (77%) white powder; melting point: 100 °C; MS (ESI pos.) *m*/*z* = 468 $[M+Na]^+$, 243 $[C_{19}H_{15}]^+$, IR (ATR) ν (cm^{-1}) = 1734 (COOH), 1698 (CO–NH–O–Trt); ^1H NMR (400 MHz, $CDCl_3$) δ = 7.46–7.28 (m, 15H,

Ar-*H*), 2.32 (t, 2H, ^3J = 7.4 Hz, CO–CH_2), 2.30 (t, 2H, ^3J = 7.5 Hz, CO–CH_2), 1.65–1.53 (m, 4H, (CH_2)$_2$), 1.37–0.97 (m, 6H, (CH_2)$_3$); ^{13}C NMR (100 MHz, $CDCl_3$) δ = 179.28, 177.81 (*C*O), 141.18, 129.23, 128.28 (Ar-*C*), 93.67 (Ph$_3$-*C*), 34.14, 31.22 (CO–*C*H$_2$), 29.26, 29.24, 29.19, 25.00, 23.78 (*C*H$_2$).

4.2.7. (*S*)-3-(4-Bromo-phenyl)-2-(7-trityloxycarbamoyl-heptanoylamino)-propionic acid methyl ester (10a). Compound **10a** was synthesized by method **C** from **9a** (1.0 g, 2.32 mmol), 50 ml anhydrous THF, NMM (759 µl, 6.94 mmol), IBCF (301 µl, 2.32 mmol) and **5** (678 mg, 2.32 mmol); yield: 1.22 g (78%) white powder; melting point: 109 °C; MS (ESI pos.) *m*/*z* = 693/695 $[M+Na]^+$, 450/452 $[C_{18}H_{24}N_2O_5Na]^+$, 243 $[C_{19}H_{15}]^+$; IR (ATR) ν (cm^{-1}) = 1745 ($COOCH_3$), 1644 (CO–NH, CO–NH–O–Trt); ^{1}H NMR (400 MHz, $CDCl_3$) δ = 7.79 (br s, 1H, Trt–O–N*H*), 7.46 (m, 2H, Ar-*H*), 7.40–7.38 (m, 2H, 3′/5′-*H*), 7.37–7.26 (m, 13H, Ar-*H*), 6.96–6.94 (m, 2H, 4′/6′-*H*), 5.92 (d, 1H, ^3J = 7.5 Hz, CO–N*H*–CH), 4.88–4.84 (m, 1H, NH–C*H*–CO), 3.72 (s, 3H, COOCH_3), 3.12 (dd, 1H, ^2J = 13.9 Hz, ^3J = 5.7 Hz, CH–CH_2–Ar), 3.03 (dd, 1H, ^2J = 13.9 Hz, ^3J = 5.7 Hz, CH–CH_2–Ar), 2.12 (t, 2H, ^3J = 7.4 Hz, CO–CH_2), 1.91–1.77 (m, 2H, CO–CH_2), 1.64–1.45 (m, 4H, (CH_2)$_2$), 1.29–1.06 (m, 4H, (CH_2)$_2$); ^{13}C NMR (100 MHz, $CDCl_3$) δ = 172.45, 171.79 (*C*O), 141.27, 134.88, 131.59, 130.90, 129.00, 128.09, 121.09 (Ar-*C*), 52.88, 52.59 (COO*C*H$_3$, NH–*C*H–CO), 37.51 (CH–*C*H$_2$–Ar), 36.52 (CO–*C*H$_2$), 28.90, 25.47 (*C*H$_2$).

4.2.8. (*S*)-3-(4-Bromo-phenyl)-2-(8-trityloxycarbamoyl-octanoylamino)-propionic acid methyl ester (10b). Compound **10b** was synthesized by method **C** from **9b** (2.82 g, 6.33 mmol), 125 ml anhydrous THF, NMM (2.69 ml, 24.1 mmol), IBCF (801 µl, 5.88 mmol) and **5** (1.8 g, 6.11 mmol); yield: 2.11 g (49%) white powder; melting point: 86 °C; MS (ESI pos.) *m*/*z* = 707/709 $[M+Na]^+$, 464/466 $[C_{19}H_{26}BrN_2O_5Na]^+$, 243 $[C_{19}H_{15}]^+$; IR (ATR) ν (cm^{-1}) = 1747 ($COOCH_3$), 1643 (CO–NH, CO–NH–O–Trt); ^{1}H NMR (300 MHz, $CDCl_3$) δ = 7.40–7.37 (m, 2H, 3′/5′-*H*), 7.36–7.27 (m, 15H, Ar-*H*), 6.96–6.94 (m, 2H, 4′/6′-*H*), 5.91 (d, 1H, ^3J = 7.8 Hz, CO–N*H*–CH), 4.89–4.83 (m, 1H, NH–C*H*–CO), 3.71 (s, 3H, COOCH_3), 3.11 (dd, 1H, ^2J = 13.9 Hz, ^3J = 5.9 Hz, CH–CH_2–Ar), 3.01 (dd, 1H, ^2J = 13.9 Hz, ^3J = 5.9 Hz, CH–CH_2–Ar), 2.13 (t, 2H, ^3J = 7.7 Hz, CO–CH_2), 1.62–1.47 (m, 4H, (CH_2)$_2$), 1.28–1.06 (m, 8H, (CH_2)$_4$); ^{13}C NMR (75.5 MHz, $CDCl_3$) δ = 172.63, 171.94 (*C*O), 141.12, 134.92, 131.62, 130.94, 129.02, 128.06, 121.10 (Ar-*C*), 52.74, 52.39 (COO*C*H$_3$, NH–*C*H–CO), 37.38 (CH–*C*H$_2$–Ar), 36.42, 33.64 (CO–*C*H$_2$), 28.84, 25.36 (*C*H$_2$).

4.2.9. (*S*)-3-Biphenyl-4-yl-2-(8-trityloxycarbamoyl-octanoylamino)-propionic acid methyl ester (11a). Compound **11a** was synthesized by method **E** from **10a** (500 mg, 0.73 mmol), benzeneboronic acid (174 mg, 1.40 mmol), tri-(*o*-tolyl)-phosphine (22 mg, 0.07 mmol), 10 ml 1,2-dimethoxyethane, 1.7 ml degassed water, palladium(II)acetate (8 mg, 0.035 mmol) and sodium carbonate (150 mg, 1.4 mmol); reaction time: five minutes; yield: 228 mg (46%) white powder; melting point: 94 °C; MS (ESI pos.) *m*/*z* = 705 $[M+Na]^+$, 462 $[C_{25}H_{31}N_2O_5Na]^+$, 243 $[C_{19}H_{15}]^+$; IR (ATR) ν (cm^{-1}) = 1745 ($COOCH_3$), 1668, 1644 (CO–NH, CO–NH–O–Trt); ^{1}H NMR (300 MHz, $CDCl_3$) δ = 7.70 (br s, 1H, Trt–O–N*H*–CO), 7.59–7.15 (m, 24H, Ar-*H*), 5.91 (d, 1H, ^3J = 7.9 Hz, N*H*–CH–CO), 4.94 (ddd, 1H, ^3J = 7.9 Hz, ^3J = 5.8 Hz, ^3J = 5.8 Hz, NH–C*H*–CO), 3.76 (s, 3H, COOCH_3), 3.21 (dd, 1H, ^2J = 14.0 Hz, ^3J = 5.8 Hz, CH–CH_2–Ar), 3.14 (dd, 1H, ^2J = 14.0 Hz, ^3J = 5.8 Hz, CH–CH_2–Ar), 2.16 (t, 2H, ^3J = 7.6 Hz, CO–CH_2), 1.65–1.51 (m, 4H, (CH_2)$_2$), 1.32–1.09 (m, 8H, (CH_2)$_4$); ^{13}C NMR (75.5 MHz, $CDCl_3$) δ = 172.63, 172.20, 170.92 (*C*O), 140.60, 139.96, 134.93, 129.65, 128.75, 128.05, 127.90, 127.89, 127.21, 126.94 (Ar-*C*), 93.20 (Ph$_3$-*C*), 52.88, 52.32 (COO*C*H$_3$, NH–*C*H–CO), 37.54 (CH–*C*H$_2$–Ar), 36.48, 31.45 (CO–*C*H$_2$), 28.85, 28.38, 28.29, 25.38, 25.08 (*C*H$_2$).

4.2.10. (*S*)-3-(4-Thiophen-2-yl-phenyl)-2-(7-trityloxycarbamoyl-heptanoylamino)-propionic acid methyl ester (11b). Compound **11b** was synthesized by method **E** from **10a** (360 mg, 0.54 mmol), 2-thienylboronic acid (134 mg, 0.87 mmol), tri-(*o*-tolyl)-phosphine (16 mg, 0.054 mmol), 7.4 ml 1,2-dimethoxyethane, 1.2 ml degassed water, palladium(II)acetate (6 mg, 0.027 mmol) and sodium carbonate (113 mg, 1.05 mmol); reaction time: five minutes; yield 175 mg (48%) white powder; melting point: 166 °C; MS (ESI pos.) *m*/*z* = 697 $[M+Na]^+$, 454 $[C_{22}H_{27}N_2O_5SNa]^+$, 243 $[C_{19}H_{15}]^+$; IR (ATR) ν (cm^{-1}) = 1748 ($COOCH_3$), 1686, 1641 (CO–NH, CO–NH–O–Trt); ^{1}H NMR (300 MHz, $CDCl_3$) δ = 7.72 (br s, 1H, Trt–O–N*H*–CO), 7.55–7.05 (m, 22H, Ar-*H*), 5.94 (d, 1H, ^3J = 7.7 Hz, N*H*–CH–CO), 4.94–4.88 (m, 1H, NH–C*H*–CO), 3.74 (s, 3H, COOCH_3), 3.17 (dd, 1H, ^2J = 14.0 Hz, ^3J = 5.8 Hz, CH–CH_2–Ar), 3.09 (dd, 1H, ^2J = 14.0 Hz, ^3J = 5.8 Hz, CH–CH_2–Ar), 2.13 (t, 2H, ^3J = 7.4 Hz, CO–CH_2), 1.89–0.96 (m, 10H, (CH_2)$_5$); ^{13}C NMR (75.5 MHz, $CDCl_3$) δ = 172.50, 172.07 (*C*O), 143.89, 141.30, 135.16, 133.26, 129.73, 128.99, 128.05, 127.98, 125.98, 124.72, 123.00 (Ar-*C*), 52.83, 52.31 (COO*C*H$_3$, NH–*C*H–CO), 37.56 (CH–*C*H$_2$–Ar), 36.31 (CO–*C*H$_2$), 28.68, 25.22 (*C*H$_2$).

4.2.11. (*S*)-3-(4-Thiophen-2-yl-phenyl)-2-(8-trityloxycarbamoyl-octanoylamino)-propionic acid methyl ester (11c). Compound **11c** was synthesized by method **E** from **10b** (400 mg, 0.58 mmol), 2-thienylboronic acid (148 mg, 1.16 mmol), tri-(*o*-tolyl)-phosphine (18 mg, 0.058 mmol), 8.3 ml 1,2-dimethoxyethane, 1.4 ml degassed water, palladium(II)acetate (7 mg, 0.029 mmol) and sodium carbonate (124 mg, 1.16 mmol); reaction time: five minutes; yield 317 mg (79%) white powder; melting point: 85 °C; MS (ESI pos.) *m*/*z* = 711 $[M+Na]^+$, 468 $[C_{23}H_{29}N_2O_5SNa]^+$, 243 $[C_{19}H_{15}]^+$; IR (ATR) ν (cm^{-1}) = 1744 ($COOCH_3$), 1675, 1644 (CO–NH, CO–NH–O–Trt); ^{1}H NMR (300 MHz, $CDCl_3$) δ = 7.75 (br s, 1H, Trt–O–N*H*–CO), 7.54–7.05 (m, 22H, Ar-*H*), 5.93 (d, 1H, ^3J = 7.9 Hz, N*H*–CH–CO), 4.95–4.88 (dpt, 1H, ^3J = 7.9 Hz, ^3J = 5.9 Hz, ^3J = 5.9 Hz, NH–C*H*–CO), 3.74 (s, 3H, COOCH_3), 3.18 (dd, 1H, ^2J = 14.0 Hz, ^3J = 5.9 Hz, CH–CH_2–Ar), 3.10 (dd, 1H, ^2J = 14.0 Hz, ^3J = 5.9 Hz, CH–CH_2–Ar), 2.15 (t, 2H, ^3J = 7.4 Hz, CO–CH_2), 1.65–1.48 (m, 4H, (CH_2)$_2$), 1.32–1.08 (m, 8H,

(CH_2)$_4$); ^{13}C NMR (75.5 MHz, $CDCl_3$) δ = 172.60, 172.09 (*C*O), 143.91, 141.10, 135.17, 133.26, 129.75, 129.00, 128.07, 127.99, 125.98, 124.74, 123.00 (Ar-*C*), 52.83, 52.33 (COO*C*H$_3$, NH–*C*H–CO), 37.58 (CH–*C*H$_2$–Ar), 36.44 (CO–*C*H$_2$), 28.85, 25.37 ((*C*H$_2$)$_5$).

4.2.12. (*S*)-3-(4-Thiophen-3-yl-phenyl)-2-(7-trityloxycarbamoyl-heptanoylamino)-propionic acid methyl ester (11d). Compound **11d** was synthesized by method **E** from **10a** (400 mg, 0.60 mmol), 3-thienylboronic acid (137 mg, 1.05 mmol), tri-(*o*-tolyl)-phosphine (17 mg, 0.053 mmol), 7.4 ml 1,2-dimethoxyethane, 1.2 ml degassed water, palladium(II)acetate (6 mg, 0.026 mmol) and sodium carbonate (113 mg, 1.05 mmol); reaction time: 5 min; yield 299 mg (74%) white powder; melting point: 173 °C; MS (ESI pos.) *m*/*z* = 697 [M+Na]$^+$, 454 [$C_{22}H_{27}N_2O_5SNa$]$^+$, 243 [$C_{19}H_{15}$]$^+$; IR (ATR) ν (cm^{-1}) = 1753 (COOCH$_3$), 1670, 1642 (CO–NH, CO–NH–O–Trt); ^{1}H NMR (300 MHz, $CDCl_3$) δ = 7.69 (br s, 1H, Trt–O–N*H*–CO), 7.53–7.10 (m, 22H, Ar-*H*), 5.89 (d, 1H, ^3J = 7.8 Hz, N*H*–CH–CO), 4.91 (dpt, 1H, ^3J = 7.8 Hz, ^3J = 5.8 Hz, ^3J = 5.8 Hz, NH–C*H*–CO), 3.74 (s, 3H, COOC*H*$_3$), 3.18 (dd, 1H, ^2J = 13.9 Hz, ^3J = 5.8 Hz, CH–C*H*$_2$–Ar), 3.10 (dd, 1H, ^2J = 13.9 Hz, ^3J = 5.8 Hz, CH–C*H*$_2$–Ar), 2.12 (t, 2H, ^3J = 7.5 Hz, CO–C*H*$_2$), 1.65–1.47 (m, 4H, (C*H*$_2$)$_2$), 1.28–1.00 (m, 6H, (C*H*$_2$)$_3$); ^{13}C NMR (75.5 MHz, $CDCl_3$) δ = 172.73, 172.37 (*C*O), 142.02, 141,35, 134.98, 134.91, 129.92, 129.24, 128.29, 126.76, 126.47, 126.39, 120.42 (Ar-*C*), 53.10, 52.56 (COO*C*H$_3$, NH–*C*H–CO), 37.81 (CH–*C*H$_2$–Ar), 36.59 (CO–*C*H$_2$), 28.93, 25.48 ((*C*H$_2$)$_4$).

4.2.13. (*S*)-3-(4-Thiophen-3-yl-phenyl)-2-(8-trityloxycarbamoyl-octanoylamino)-propionic acid methyl ester (11e). Compound **11e** was synthesized by method **E** from **10b** (400 mg, 0.58 mmol), 3-thienylboronic acid (150 mg, 1.16 mmol), tri-(*o*-tolyl)-phosphine (18 mg, 0.058 mmol), 8.2 ml 1,2-dimethoxyethane, 1.3 ml degassed water, palladium(II)acetate (7 mg, 0.029 mmol) and sodium carbonate (125 mg, 1.16 mmol); reaction time: 5 min; yield 337 mg (84%) white powder; melting point: 137 °C; MS (ESI pos.) *m*/*z* = 711 [M+Na]$^+$, 468 [$C_{23}H_{29}N_2O_5SNa$]$^+$, 243 [$C_{19}H_{15}$]$^+$; IR (ATR) ν (cm^{-1}) = 1742 (COOCH$_3$), 1649 (CO–NH, CO–NH–O–Trt); ^{1}H NMR (300 MHz, $CDCl_3$) δ = 7.71 (br s, 1H, Trt–O–N*H*–CO), 7.54–7.51 (m, 2H, 3′/5′-*H*), 7.43 (pt, 1H, ^3J = 2.1 Hz, ^3J = 2.1 Hz, 2″-*H*), 7.37–7.00 (m, 17H, Ar-*H*), 7.14–7.11 (m, 2H, 2′/6′-*H*), 5.90 (d, 1H, ^3J = 7.9 Hz, N*H*–CH–CO), 4.91 (dpt, 1H, ^3J = 7.9 Hz, ^3J = 5.8 Hz, ^3J = 5.8 Hz, NH–C*H*–CO), 3.75 (s, 3H, COOC*H*$_3$), 3.19 (dd, 1H, ^2J = 13.9 Hz, ^3J = 5.8 Hz, CH–C*H*$_2$–Ar), 3.11 (dd, 1H, ^2J = 13.9 Hz, ^3J = 5.8 Hz, CH–C*H*$_2$–Ar), 2.16 (t, 2H, ^3J = 7.6 Hz, CO–C*H*$_2$), 1.89–0.97 (m, 12H, (C*H*$_2$)$_6$); ^{13}C NMR (75.5 MHz, $CDCl_3$) δ = 172.55, 172.14 (*C*O), 141.80, 141,19, 134.76, 134.68, 129.69, 129.00, 128.05, 126.52, 126.25, 126.15, 120.17 (Ar-*C*), 52.86, 52.31 (COO*C*H$_3$, NH–*C*H–CO), 37.60 (CH–*C*H$_2$–Ar), 36.46, 31.56 (CO–*C*H$_2$), 28.85, 25.38 (*C*H$_2$).

4.2.14. (*S*)-3-(4-Furan-2-yl-phenyl)-2-(7-trityloxycarbamoyl-heptanoylamino)-propionic acid methyl ester (11f). Compound **11f** was synthesized by method **E** from **10a** (400 mg, 0.60 mmol), 2-furanboronic acid (133 mg, 1.20 mmol), tri-(*o*-tolyl)-phosphine (19 mg, 0.06 mmol), 8.4 ml 1,2-dimethoxyethane, 1.4 ml degassed water, palladium(II)acetate (7 mg, 0.03 mmol) and sodium carbonate (128 mg, 1.20 mmol); reaction time: five minutes; yield 261 mg (66%) white powder; melting point: 87 °C; MS (ESI pos.) *m*/*z* = 681 [M+Na]$^+$, 438 [$C_{22}H_{27}N_2O_6Na$]$^+$, 243 [$C_{19}H_{15}$]$^+$; IR (ATR) ν (cm^{-1}) = 1744 (COOCH$_3$), 1640 (CO–NH, CO–NH–O–Trt); ^{1}H NMR (300 MHz, $CDCl_3$) δ = 7.60–7.57 (m, 2H, 3′/5′-*H*), 7.44 (m, 1H, 5″-*H*), 7.33 (m, 15H, Ar-*H*), 7.11–7.08 (m, 2H, 2′/6′-*H*), 6.62–6.61 (m, 1H, 3″-*H*), 6.46–6.44 (m, 1H, 4″-*H*), 5.86 (d, 1H, ^3J = 7.8 Hz, N*H*–CH–CO), 4.92–4.86 (m, 1H, NH–C*H*–CO), 3.73 (s, 3H, COOC*H*$_3$), 3.16 (dd, 1H, ^2J = 13.9 Hz, ^3J = 5.9 Hz, CH–C*H*$_2$–Ar), 3.08 (dd, 1H, ^2J = 13.9 Hz, ^3J = 5.9 Hz, CH–C*H*$_2$–Ar), 2.12 (t, 2H, ^3J = 7.6 Hz, CO–C*H*$_2$), 1.81–0.96 (m, 10H, (C*H*$_2$)$_5$); ^{13}C NMR (75.5 MHz, $CDCl_3$) δ = 172.48, 172.10 (*C*O), 153.67 (2″-*C*), 142.03, 141.20, 134.99, 129.84, 129.57, 129.02, 128.07, 123.95 (Ar-*C*), 111.64 (3″-*C*), 104.97 (4″-*C*), 52.89, 52.32 (COO*C*H$_3$, NH–*C*H–CO), 37.73 (CH–*C*H$_2$–Ar), 36.37 (CO–*C*H$_2$), 28.71, 25.26 (*C*H$_2$).

4.2.15. (*S*)-3-(4-Furan-2-yl-phenyl)-2-(8-trityloxycarbamoyl-octanoylamino)-propionic acid methyl ester (11g). Compound **11g** was synthesized by method **E** from **10b** (400 mg, 0.58 mmol), 2-furanboronic acid (131 mg, 1.16 mmol), tri-(*o*-tolyl)-phosphine (18 mg, 0.058 mmol), 8.2 ml 1,2-dimethoxyethane, 1.4 ml degassed water, palladium(II)acetate (7 mg, 0.03 mmol) and sodium carbonate (126 mg, 1.16 mmol); reaction time: 5 min; yield 324 mg (83%) white powder; melting point: 93 °C; MS (ESI pos.) *m*/*z* = 695 [M+Na]$^+$, 452 [$C_{23}H_{29}N_2O_6Na$]$^+$, 243 [$C_{19}H_{15}$]$^+$; IR (ATR) ν (cm^{-1}) = 1738 (COOCH$_3$), 1668, 1644 (CO–NH, CO–NH–O–Trt); ^{1}H NMR (300 MHz, $CDCl_3$) δ = 7.71 (br s, 1H, Trt–O–N*H*–CO), 7.61–7.58 (m, 2H, 3′/5′-*H*), 7.44 (m, 1H, 5″-*H*), 7.34 (m, 15H, Ar-*H*), 7.12–7.10 (m, 2H, 2′/6′-*H*), 6.63 (d, 1H, ^3J = 3.3 Hz, ^4J = 0.6 Hz, 3″-*H*), 6.46 (d, 1H, ^3J = 3.3 Hz, ^3J = 1.8 Hz, 4″-*H*), 5.90 (d, 1H, ^3J = 7.8 Hz, N*H*–CH–CO), 4.91 (dpt, 1H, ^3J = 7.8 Hz, ^3J = 5.9 Hz, ^3J = 5.9 Hz, NH–C*H*–CO), 3.74 (s, 3H, COOC*H*$_3$), 3.17 (dd, 1H, ^2J = 13.9 Hz, ^3J = 5.9 Hz, CH–C*H*$_2$–Ar), 3.10 (dd, 1H, ^2J = 13.9 Hz, ^3J = 5.9 Hz, CH–C*H*$_2$–Ar), 2.15 (t, 2H, ^3J = 7.5 Hz, CO–C*H*$_2$), 1.65–1.49 (m, 4H, (C*H*$_2$)$_2$), 1.27–1.00 (m, 8H, (C*H*$_2$)$_4$); ^{13}C NMR (75.5 MHz, $CDCl_3$) δ = 172.54, 172.10 (*C*O), 153.65 (2″-*C*), 142.02, 141,30, 134.99, 129.81, 129.56, 129.01, 128.05, 123.93 (Ar-*C*), 111.63 (3″-*C*), 104.94 (4″-*C*), 52.86, 52.31 (COO*C*H$_3$, NH–*C*H–CO), 37.72 (CH–*C*H$_2$–Ar), 36.45 (CO–*C*H$_2$), 28.84, 25.38 (*C*H$_2$).

4.2.16. (*S*)-3-(4-Furan-3-yl-phenyl)-2-(7-trityloxycarbamoyl-heptanoylamino)-propionic acid methyl ester (11h). Compound **11h** was synthesized by method **E** from **10a** (400 mg, 0.60 mmol), 3-furanboronic acid (133 mg, 1.20 mmol), tri-(*o*-tolyl)-phosphine (19 mg, 0.06 mmol), 8.4 ml 1,2-dimethoxyethane, 1.4 ml degassed water, palladium(II)acetate (7 mg, 0.03 mmol) and sodium carbonate (128 mg, 1.20 mmol); reaction time: 5 min; 316 mg (80%) white powder; melting point: 110 °C; MS (ESI pos.) *m*/*z* = 681 [M+Na]$^+$, 438 [$C_{22}H_{27}N_2O_6Na$]$^+$, 243 [$C_{19}H_{15}$]$^+$; IR (ATR) ν(cm^{-1}) = 1750 (COOCH$_3$), 1666, 1641 (CO–NH, CO–NH–O–Trt); ^{1}H NMR (300 MHz,

$CDCl_3$) δ = 7.72–7.71 (m, 1H, 2″-*H*), 7.46 (pt, 1H, ^3J = 1.7 Hz, ^4J = 1.7 Hz, 5″-*H*), 7.42–7.40 (m, 2H, 3′/5′-*H*), 7.34 (m, 15H, Ar-*H*), 7.11–7.08 (m, 2H, 2′/6′-*H*), 6.68 (dd, 1H, ^3J = 1.7 Hz, ^4J = 0.8 Hz, 4″-*H*), 5.90 (d,1H, ^3J = 7.7 Hz, N*H*–CH–CO), 4.89 (dpt, 1H, ^3J = 7.7 Hz, ^3J = 5.9 Hz, ^3J = 5.9 Hz, NH–C*H*–CO), 3.74 (s, 3H, COOCH_3), 3.17 (dd, 1H, ^2J = 14.0 Hz, ^3J = 5.9 Hz, CH–CH_2–Ar), 3.09 (dd, 1H, ^2J = 14.0 Hz, ^3J = 5.9 Hz, CH–CH_2–Ar), 2.13 (t, 2H, ^3J = 7.5 Hz, CO–CH_2), 1.90–1.00 (m, 10H, (CH_2)$_5$); ^{13}C NMR (75.5 MHz, $CDCl_3$) δ = 172.50, 172.13 (*C*O), 143.67 (5″-*C*), 141.02, 138.45, 134.59, 131.28, 129.68, 129.00, 128.05, 126.02, 125.97 (Ar-*C*), 108.70 (4″-*C*), 52.88, 52.31 (COO*C*H_3, NH–*C*H–CO), 37.60 (CH–*C*H_2–Ar), 36.34 (CO–*C*H_2), 28.68, 25.23 (*C*H_2).

4.2.17. (*S*)-3-(4-Furan-3-yl-phenyl)-2-(8-trityloxycarbamoyl-octanoylamino)-propionic acid methyl ester (11i). Compound **11i** was synthesized by method **E** from **10b** (400 mg, 0.58 mmol), 3-furanboronic acid (131 mg, 1.16 mmol), tri-(*o*-tolyl)-phosphine (18 mg, 0.058 mmol), 8.2 ml 1,2-dimethoxyethane, 1.4 ml degassed water, palladium(II)acetate (7 mg, 0.03 mmol) and sodium carbonate (126 mg, 1.16 mmol); reaction time: five minutes; yield 335 mg (86%) white powder; melting point: 143 °C; MS (ESI pos.) *m*/*z* = 695 $[M+Na]^+$, 452 $[C_{23}H_{29}N_2O_6Na]^+$, 243 $[C_{19}H_{15}]^+$; IR (ATR) ν (cm^{-1}) = 1741 ($COOCH_3$), 1668, 1645 (CO–NH, CO–NH–O–Trt); ^{1}H NMR (300 MHz, $CDCl_3$) δ = 7.71 (dd, 1H, ^4J = 1.7 Hz, ^4J = 0.9 Hz, 2″-*H*), 7.46 (pt, 1H, ^3J = 1.7 Hz, ^4J = 1.7 Hz, 5″-*H*), 7.42–7.39 (m, 2H, 3′/5′-*H*), 7.34 (m, 15H, Ar-*H*), 7.11–7.08 (m, 2H, 2′/6′-*H*), 6.68 (dd, 1H, ^3J = 1.7 Hz, ^4J = 0.9 Hz, 4″-*H*), 5.91 (d, 1H, ^3J = 7.8 Hz, N*H*–CH–CO), 4.89 (dpt, 1H, ^3J = 7.8 Hz, ^3J = 5.9 Hz, ^3J = 5.9 Hz, NH–C*H*-CO), 3.74 (s, 3H, COOCH_3), 3.17 (dd, 1H, ^2J = 13.9 Hz, ^3J = 5.9 Hz, CH–CH_2–Ar), 3.10 (dd, 1H, ^2J = 13.9 Hz, ^3J = 5.9 Hz, CH–CH_2–Ar), 2.15 (t, 2H, ^3J = 7.5 Hz, CO–CH_2), 1.66–1.53 (m, 4H, (CH_2)$_2$), 1.29–1.01 (m, 8H, (CH_2)$_4$); ^{13}C NMR (75.5 MHz, $CDCl_3$) δ = 172.08, 171.65 (*C*O), 143.19 (5″-*C*), 140.59, 137.93, 134.09, 130.76, 129.19, 128.51, 127.58, 125.52, 125.47 (Ar-*C*), 108.21 (4″-*C*), 52.37, 51.84 (COO*C*H_3, NH–*C*H–CO), 37.10 (CH–*C*H_2–Ar), 35.96 (CO–*C*H_2), 28.38, 24.89 (*C*H_2).

4.2.18. (*S*)-3-[1,1′:4′,1″]Terphenyl-4-yl-2-(7-trityloxycarbamoyl-heptanoylamino)-propionic acid methyl ester (11j). Compound **11j** was synthesized by method **E** from **10a** (400 mg, 0.60 mmol), 4-biphenylboronic acid (176 mg, 0.90 mmol), tri-(*o*-tolyl)-phosphine (19 mg, 0.06 mmol), 8.4 ml 1,2-dimethoxyethane, 1.4 ml degassed water, palladium(II)acetate (7 mg, 0.03 mmol) and sodium carbonate (128 mg, 1.20 mmol); reaction time: ten minutes; the crude product was purified by flash chromatography on silica gel using ethyl acetate, cyclohexane and dichloromethane (2:1:1) as mobile phase; yield 285 mg (64%) white powder; melting point: 205 °C; MS (ESI pos.) *m*/*z* = 767 $[M+Na]^+$, 524 $[C_{30}H_{33}N_2O_5Na]^+$, 243 $[C_{19}H_{15}]^+$; IR (ATR) ν (cm^{-1}) = 1737 ($COOCH_3$), 1669, 1644 (CO–NH, CO–NH–O–Trt); ^{1}H NMR (300 MHz, $CDCl_3$) δ = 7.63–7.14 (m, 28H, Ar-*H*), 5.91 (d, 1H, ^3J = 7.8 Hz, CO–N*H*–CH), 4.94–4.88 (m, 1H, NH–C*H*–CO), 3.73 (s, 3H, COOCH_3), 3.19 (dd, 1H, ^2J = 13.9 Hz, ^3J = 5.8 Hz, CH–CH_2–Ar), 3.14 (dd, 1H, ^2J = 13.9 Hz, ^3J = 5.8 Hz, CH–CH_2–Ar), 2.12 (t, 2H, ^3J = 7.4 Hz, CO–CH_2), 1.65–0.93 (m, 10H, (CH_2)$_5$); ^{13}C NMR (75.5 MHz, $CDCl_3$) δ = 172.54, 172.16 (*C*O), 141.12, 140.63, 140.15, 139.49, 139.45, 135.07, 129.72, 129.00, 128.79, 128.04, 127.48, 127.34, 127.29, 127.10, 127.00 (Ar-*C*), 52.91, 52.33 (COO*C*H_3, NH–*C*H–CO), 37.56 (CH–*C*H_2–Ar), 36.35 (CO–*C*H_2), 28.69, 25.24 (*C*H_2).

4.2.19. (*S*)-3-[1,1′:4′,1″]Terphenyl-4-yl-2-(8-trityloxycarbamoyl-octanoylamino)-propionic acid methyl ester (11k). Compound **11k** was synthesized by method **E** from **10b** (400 mg, 0.58 mmol), 4-biphenylboronic acid (172 mg, 0.87 mmol), tri-(*o*-tolyl)-phosphine (18 mg, 0.058 mmol), 8.2 ml 1,2-dimethoxyethane, 1.4 ml degassed water, palladium(II)acetate (7 mg, 0.03 mmol) and sodium carbonate (124 mg, 1.16 mmol); reaction time: ten minutes; the crude product was purified by flash chromatography on silica gel using ethyl acetate, cyclohexane and dichloromethane (2:1:1) as mobile phase; yield 370 mg (84%) white powder; melting point: 184 °C; MS (ESI pos.) *m*/*z* = 781 $[M+Na]^+$, 538 $[C_{31}H_{35}N_2O_5Na]^+$, 243 $[C_{19}H_{15}]^+$; IR (ATR) ν (cm^{-1}) = 1739 ($COOCH_3$), 1669, 1647 (CO–NH, CO–NH–O–Trt); ^{1}H NMR (300 MHz, $CDCl_3$) δ = 7.66–7.16 (m, 28H, Ar-*H*), 5.93 (d, 1H, ^3J = 7.7 Hz, CO–N*H*–CH), 4.96 (dpt, 1H, ^3J = 7.7 Hz, ^3J = 5.9 Hz, ^3J = 5.9 Hz, NH–C*H*–CO), 3.76 (s, 3H, COOCH_3), 3.22 (dd, 1H, ^2J = 13.9 Hz, ^3J = 5.9 Hz, CH–CH_2–Ar), 3.14 (dd, 1H, ^2J = 13.9 Hz, ^3J = 5.9 Hz, CH–CH_2–Ar), 2.17 (t, 2H, ^3J = 7.6 Hz, CO–CH_2), 1.69–0.96 (m, 12H, (CH_2)$_6$); ^{13}C NMR (75.5 MHz, $CDCl_3$) δ = 172.59, 172.16 (*C*O), 141.12, 140.61, 140.15, 139.48, 139.43, 135.05, 129.73, 129.01, 128.80, 128.05, 127.49, 127.35, 127.28, 127.09, 127.00 (Ar-*C*), 93.34 (Ph_3-*C*), 52.90, 52.34 (COO*C*H_3, NH–*C*H–CO), 37.58 (CH–*C*H_2–Ar), 36.47 (CO–*C*H_2), 28.85, 25.39 (*C*H_2).

4.2.20. (*S*)-3-(4-Naphthalen-2-yl-phenyl)-2-(7-trityloxycarbamoyl-heptanoylamino)-propionic acid methyl ester (11l). Compound **11l** was synthesized by method **E** from **10a** (400 mg, 0.60 mmol), 2-naphthylboronic acid (181 mg, 1.06 mmol), tri-(*o*-tolyl)-phosphine (17 mg, 0.055 mmol), 7.4 ml 1,2-dimethoxyethane, 1.2 ml degassed water, palladium(II)acetate (6 mg, 0.026 mmol) and sodium carbonate (113 mg, 1.06 mmol); reaction time: ten minutes; yield 334 mg (77%) white powder; melting point: 155 °C; MS (ESI pos.) *m*/*z* = 741 $[M+Na]^+$, 498 $[C_{28}H_{31}N_2O_5Na]^+$, 243 $[C_{19}H_{15}]^+$; IR (ATR) ν (cm^{-1}) = 1739 ($COOCH_3$), 1670, 1645 (CO–NH, CO–NH–O–Trt); ^{1}H NMR (300 MHz, $CDCl_3$) δ = 8.02 (br s, 1H, Trt–O–N*H*–CO), 7.92–7.19 (m, 26H, Ar-*H*), 5.94 (d, 1H, ^3J = 7.8 Hz, CO–N*H*–CH), 4.96 (dpt, 1H, ^3J = 7.8 Hz, ^3J = 5.8 Hz, ^3J = 5.8 Hz, NH–C*H*–CO), 3.77 (s, 3H, COOCH_3), 3.23 (dd, 1H, ^2J = 13.9 Hz, ^3J = 5.8 Hz, CH–CH_2–Ar), 3.16 (dd, 1H, ^2J = 13.9 Hz, ^3J = 5.8 Hz, CH–CH_2–Ar), 2.15 (t, 2H, ^3J = 7.6 Hz, CO–CH_2), 1.59–1.00 (m, 10H, (CH_2)$_5$); ^{13}C NMR (75.5 MHz, $CDCl_3$) δ = 172.54, 172.15 (*C*O), 141.13, 139.86, 137.92, 135.06, 133.66, 132.62, 129.76, 129.00, 128.42, 128.15, 128.05, 127.61, 127.48, 126.29, 125.94, 125.62, 125.34 (Ar-*C*), 93.50 (Ph_3-*C*), 52.92, 52.35 (COO*C*H_3, NH–*C*H–CO), 37.56 (CH–*C*H_2–Ar), 36.37 (CO–*C*H_2), 28.72, 25.25 (*C*H_2).

4.2.21. (*S*)-3-(4-Naphthalen-2-yl-phenyl)-2-(8-trityloxycarbamoyl-octanoylamino)-propionic acid methyl ester (11m). Compound **11m** was synthesized by method **E** from **10b** (400 mg, 0.58 mmol), 2-naphthylboronic acid (149 mg, 0.87 mmol), tri-(*o*-tolyl)-phosphine (18 mg, 0.058 mmol), 8.2 ml 1,2-dimethoxyethane, 1.4 ml degassed water, palladium(II)acetate (7 mg, 0.029 mmol) and sodium carbonate (124 mg, 1.16 mmol); reaction time: ten minutes; yield 367 mg (86%) white powder; melting point: 97 °C; MS (ESI pos.) m/z = 755 $[M+Na]^+$, 512 $[C_{29}H_{33}N_2O_5Na]^+$, 243 $[C_{19}H_{15}]^+$; IR (ATR) ν (cm^{-1}) = 1744 ($COOCH_3$), 1652, 1615 (CO–NH, CO–NH–O–Trt); ^1H NMR (300 MHz, $CDCl_3$) δ = 8.00 (br s, 1H, Trt–O–N*H*–CO), 7.91–7.19 (m, 26H, Ar-*H*), 5.94 (d, 1H, ^3J = 7.8 Hz, CO–N*H*–CH), 4.96 (dpt, 1H, ^3J = 7.8 Hz, ^3J = 5.8 Hz, ^3J = 5.8 Hz, NH–C*H*–CO), 3.76 (s, 3H, $COOCH_3$), 3.23 (dd, 1H, ^2J = 13.9 Hz, ^3J = 5.8 Hz, CH–CH_2–Ar), 3.16 (dd, 1H, ^2J = 13.9 Hz, ^3J = 5.8 Hz, CH–CH_2–Ar), 2.17 (t, 2H, ^3J = 7.6 Hz, CO–CH_2), 1.59–0.98 (m, 12H, $(CH_2)_6$); ^{13}C NMR (75.5 MHz, $CDCl_3$) δ = 172.59, 172.16 (*C*O), 141.22, 139.85, 137.92, 135.07, 133.65, 132.61, 129.77, 129.00, 128.43, 128.15, 128.04, 127.61, 127.47, 126.30, 125.94, 125.61, 125.34 (Ar-*C*), 93.34 (Ph_3-*C*), 52.91, 52.34 ($COOCH_3$, NH–*C*H–CO), 37.58 (CH–*C*H_2–Ar), 36.47 (CO–*C*H_2), 28.85, 25.39 (*C*H_2).

4.2.22. (*S*)-3-Biphenyl-4-yl-2-(8-hydroxycarbamoyl-octanoylamino)-propionic acid methyl ester (4a). Compound **4a** was synthesized by method **F** from **11a** (200 mg, 0.29 mmol), 2.0 ml dichloromethane, TFA and TES; yield 88 mg (69%) grey powder; melting point: 130 °C; MS (ESI pos.) m/z = 463 $[M+Na]^+$; IR (ATR) ν (cm^{-1}) = 1751 ($COOCH_3$), 1640 (CO–NH, CO–NH–OH); ^1H NMR (300 MHz, DMSO-d_6) δ = 10.28 (s, 1H, *H*O–NH–CO), 8.61 (s, 1H, HO–N*H*–CO), 8.25 (d, 1H, ^3J = 7.9 Hz, N*H*–CH–CO), 7.64–7.28 (m, 9H, Ar-*H*), 4.55–4.47 (m, 1H, NH–C*H*–CO), 3.61 (s, 3H, $COOCH_3$), 3.07 (dd, 1H, ^2J = 13.8 Hz, ^3J = 5.3 Hz, CH–CH_2–Ar), 2.91 (dd, 1H, ^2J = 13.8 Hz, ^3J = 9.8 Hz, CH–CH_2–Ar), 2.04 (t, 2H, ^3J = 7.2 Hz, CO–CH_2), 1.88 (t, 2H, ^3J = 7.4 Hz, CO–CH_2), 1.46–1.34 (m, 4H, $(CH_2)_2$), 1.20–1.08 (m, 6H, $(CH_2)_2$); ^{13}C NMR (75.5 MHz, DMSO-d_6) δ = 172.27, 172.15, 169.05 (*C*O), 139.81, 138.27, 136.59, 129.59, 128.84, 126.41, 126.37, 125.81 (Ar-*C*), 53.25, 51.78 ($COOCH_3$, NH–*C*H–CO), 36.24 (CH–*C*H_2–Ar), 34.94, 32.19 (CO–*C*H_2), 28.42, 28.29, 25.05 (*C*H_2).

4.2.23. (*S*)-2-(7-Hydroxycarbamoyl-heptanoylamino)-3-(4-thiophen-2-yl-phenyl)-propionic acid methyl ester (4b). Compound **4b** was synthesized by method **F** from **11b** (160 mg, 0.24 mmol), 1.6 ml dichloromethane, TFA and TES; yield 57 mg (55%) grey powder; melting point: 106 °C; MS (ESI pos.) m/z = 433 $[M+H]^+$; IR (ATR) ν (cm^{-1}) = 1736 ($COOCH_3$), 1645, 1629 (CO–NH, CO–NH–OH); ^1H NMR (300 MHz, DMSO-d_6) δ = 10.28 (s, 1H, *H*O–NH–CO), 8.61 (s, 1H, HO–N*H*–CO), 8.24 (d, 1H, ^3J = 8.0 Hz, N*H*–CH–CO), 7.57–7.54 (m, 2H, 3′/5′-*H*), 7.49 (dd, 1H, ^3J = 5.1 Hz, ^4J = 1.0 Hz, 5″-*H*), 7.46 (dd, 1H, ^3J = 3.7 Hz, ^4J = 1.0 Hz, 3″-*H*), 7.25–7.23 (m, 2H, 2′/6′-*H*), 7.12–7.09 (dd, 1H, ^3J = 5.1 Hz, ^3J = 3.7 Hz, 4″-*H*), 4.49 (ddd, 1H, ^3J = 9.5 Hz, ^3J = 8.0 Hz, ^3J = 5.5 Hz, NH–C*H*–CO), 3.60 (s, 3H, $COOCH_3$), 3.03 (dd, 1H, ^2J = 13.8 Hz, ^3J = 5.5 Hz, CH–CH_2–Ar), 2.91–2.84 (dd, 1H, ^2J = 13.8 Hz, ^3J = 9.5 Hz, CH–CH_2–Ar), 2.03 (t, 2H, ^3J = 7.3 Hz, CO–CH_2), 1.88 (t, 2H, ^3J = 7.4 Hz, CO–CH_2), 1.43–1.31 (m, 4H, $(CH_2)_2$), 1.21–1.04 (m, 4H, $(CH_2)_2$); ^{13}C NMR (75.5 MHz, DMSO-d_6) δ = 172.23, 172.08, 169.04 (*C*O), 143.16, 136.76, 132.02, 129.74, 128.38, 125.80, 125.17, 123.36 (Ar-*C*), 53.20, 51.78 ($COOCH_3$, NH–*C*H–CO), 36.28 (CH–*C*H_2–Ar), 34.90, 32.18 (CO–*C*H_2), 28.29, 28.14, 24.99, 24.93 (*C*H_2).

4.2.24. (*S*)-2-(8-Hydroxycarbamoyl-octanoylamino)-3-(4-thiophen-2-yl-phenyl)-propionic acid methyl ester (4c). Compound **4c** was synthesized by method **F** from **11c** (300 mg, 0.44 mmol), 3.0 ml dichloromethane, TFA and TES; yield 152 mg (77%) grey powder; melting point: 142 °C; MS (ESI pos.) m/z = 469 $[M+Na]^+$, 447 $[M+H]^+$; IR (ATR) ν (cm^{-1}) = 1750 ($COOCH_3$), 1639, 1625 (CO–NH, CO–NH–OH); ^1H NMR (300 MHz, DMSO-d_6) δ = 10.28 (s, 1H, *H*O–NH–CO), 8.61 (s, 1H, HO–N*H*–CO), 8.22 (d, 1H, ^3J = 8.0 Hz, N*H*–CH–CO), 7.55–7.53 (m, 2H, 3′/5′-*H*), 7.49 (dd, 1H, ^3J = 5.1 Hz, ^4J = 1.1 Hz, 5″-*H*), 7.45 (dd, 1H, ^3J = 3.6 Hz, ^4J = 1.1 Hz, 3″-*H*), 7.25–7.22 (m, 2H, 2′/6′-*H*), 7.10 (dd, 1H, ^3J = 5.1 Hz, ^3J = 3.6 Hz, 4″-*H*), 4.49 (ddd, 1H, ^3J = 9.6 Hz, ^3J = 8.0 Hz, ^3J = 5.2 Hz, NH–C*H*–CO), 3.60 (s, 3H, $COOCH_3$), 3.03 (dd, 1H, ^2J = 13.7 Hz, ^3J = 5.2 Hz, CH–CH_2–Ar), 2.86 (dd, 1H, ^2J = 13.7 Hz, ^3J = 9.6 Hz, CH–CH_2–Ar), 2.02 (t, 2H, ^3J = 7.3 Hz, CO–CH_2), 1.87 (t, 2H, ^3J = 7.4 Hz, CO–CH_2), 1.45–1.32 (m, 4H, $(CH_2)_2$), 1.21–1.05 (m, 6H, $(CH_2)_3$); ^{13}C NMR (75.5 MHz, DMSO-d_6) δ = 172.24, 172.09, 169.07 (*C*O–NH), 143.18, 136.76, 132.02, 129.74, 128.39, 125.30 125.16, 123.34 (Ar-*C*), 53.17, 51.79 ($COOCH_3$, NH–*C*H–CO), 36.29 (CH–*C*H_2–Ar), 34.94, 32.20 (CO–*C*H_2), 28.44, 28.29, 25.06 (*C*H_2).

4.2.25. (*S*)-2-(7-Hydroxycarbamoyl-heptanoylamino)-3-(4-thiophen-3-yl-phenyl)-propionic acid methyl ester (4d). Compound **4d** was synthesized by method **F** from **11d** (280 mg, 0.41 mmol), 2.8 ml dichloromethane, TFA and TES; yield 110 mg (62%) grey powder; melting point: 128 °C; MS (ESI pos.) m/z = 455 $[M+Na]^+$; IR (ATR) ν (cm^{-1}) = 1737 ($COOCH_3$), 1645, 1630 (CO–NH, CO–NH–OH); ^1H NMR (300 MHz, DMSO-d_6) δ = 10.28 (s, 1H, *H*O–NH–CO), 8.62 (s, 1H, HO–N*H*–CO), 8.24 (d, 1H, ^3J = 7.9 Hz, N*H*–CH–CO), 7.82 (dd, 1H, ^4J = 2.9 Hz, ^4J = 1.3 Hz, 2″-*H*), 7.63–7.60 (m, 2H, 3′/5′-*H*), 7.61–7.59 (m, 1H, 5″-*H*), 7.52 (dd, 1H, ^3J = 5.0 Hz, ^4J = 1.3 Hz, 4″-*H*), 7.25–7.22 (m, 2H, 2′/6′-*H*), 4.52–4.44 (m, 1H, NH–C*H*–CO), 3.60 (s, 3H, $COOCH_3$), 3.03 (dd, 1H, ^2J = 13.8 Hz, ^3J = 5.3 Hz, CH–CH_2–Ar), 2.88 (dd, 1H, ^2J = 13.8 Hz, ^3J = 9.5 Hz, CH–CH_2–Ar), 2.04 (t, 2H, ^3J = 7.4 Hz, CO–CH_2), 1.88 (t, 2H, ^3J = 7.4 Hz, CO–CH_2), 1.45–1.32 (m, 4H, $(CH_2)_2$), 1.21–1.06 (m, 4H, $(CH_2)_2$); ^{13}C NMR (75.5 MHz, DMSO-d_6) δ = 172.23, 171.15, 169.05 (*C*O–NH), 141.15, 136.16, 133.37, 129.51, 126.91, 126.02, 125.81, 120.49 (Ar-*C*), 53.28, 51.75 ($COOCH_3$, NH–*C*H–CO), 36.30 (CH–*C*H_2–Ar), 34.91, 32.18 (CO–*C*H_2), 28.29, 28.15, 25.00, 24.94 (*C*H_2).

4.2.26. (*S*)-2-(8-Hydroxycarbamoyl-octanoylamino)-3-(4-thiophen-3-yl-phenyl)-propionic acid methyl ester (4e). Compound **4e** was synthesized by method **F** from **11e** (300 mg, 0.44 mmol), 3.0 ml dichloromethane, TFA and TES; yield 157 mg (80%) grey powder; melting point: 124 °C; MS (ESI pos.) *m*/*z* = 447 $[M+H]^+$; IR (ATR) *v* (cm^{-1}) = 1750 ($COOCH_3$), 1639 (CO–NH, CO–NH–OH); ^1H NMR (300 MHz, DMSO-d_6) δ = 10.28 (s, 1H, *H*O–NH–CO), 8.61 (s, 1H, HO–N*H*–CO), 8.23 (d, 1H, ^3J = 8.0 Hz, N*H*–CH–CO), 7.81 (dd, 1H, ^4J = 2.8 Hz, ^4J = 1.3 Hz, 2″-*H*), 7.63–7.60 (m, 2H, 3′/5′-*H*), 7.61–7.59 (m, 1H, 5″-*H*), 7.52 (dd, 1H, ^3J = 5.0 Hz, ^4J = 1.3 Hz, 4″-*H*), 7.25–7.22 (m, 2H, 2′/6′-*H*), 4.49 (ddd, 1H, ^3J = 9.5 Hz, ^3J = 8.0 Hz, ^3J = 5.4 Hz, NH–C*H*–CO), 3.60 (s, 3H, $COOCH_3$), 3.04 (dd, 1H, ^2J = 13.7 Hz, ^3J = 5.4 Hz, CH–CH_2–Ar), 2.88 (dd, 1H, ^2J = 13.7 Hz, ^3J = 9.5 Hz, CH–CH_2–Ar), 2.04 (t, 2H, ^3J = 7.3 Hz, CO–CH_2), 1.88 (t, 2H, ^3J = 7.3 Hz, CO–CH_2), 1.46–1.32 (m, 4H, (CH_2)$_2$), 1.21–1.05 (m, 6H, (CH_2)$_2$); ^{13}C NMR (75.5 MHz, DMSO-d_6) δ = 172.23, 172.14, 169.07 (*C*O), 141.16, 136.15, 133.36, 129.50, 126.91, 126.00 125.80, 120.47 (Ar-*C*), 53.25, 51.75 (COO*C*H_3, NH–*C*H–CO), 36.30 (CH–*C*H_2–Ar), 34.93, 32.19 (CO–*C*H_2), 28.44, 28.42, 28.29, 25.06, 25.05 ((CH_2)$_5$).

4.2.27. (*S*)-3-(4-Furan-2-yl-phenyl)-2-(7-hydroxycarbamoyl-heptanoylamino)-propionic acid methyl ester (4f). Compound **4f** was synthesized by method **F** from **11f** (225 mg, 0.34 mmol), 2.2 ml dichloromethane, TFA and TES; yield 75 mg (53%) grey powder; melting point: 137 °C; MS (ESI pos.) *m*/*z* = 417 $[M+H]^+$; IR (ATR) *v* (cm^{-1}) = 1736 ($COOCH_3$), 1646 (CO–NH, CO–NH–OH); ^1H NMR (300 MHz, DMSO-d_6) δ = 10.29 (s, 1H, *H*O–NH–CO), 8.62 (s, 1H, HO–N*H*–CO), 8.23 (d, 1H, ^3J = 7.9 Hz, N*H*–CH–CO), 7.70 (m, 1H, 5″-*H*), 7.61–7.58 (m, 2H, 3′/5′-*H*), 7.26–7.24 (m, 2H, 2′/6′-*H*), 6.89–6.88 (m, 1H, 3″-*H*), 6.57–6.55 (m, 1H, 4″-*H*), 4.52–4.45 (m, 1H, NH–C*H*–CO), 3.60 (s, 3H, $COOCH_3$), 3.03 (dd, 1H, ^2J = 13.8 Hz, ^3J = 5.3 Hz, CH–CH_2–Ar), 2.88 (dd, 1H, ^2J = 13.8 Hz, ^3J = 9.6 Hz, CH–CH_2–Ar), 2.03 (t, 2H, ^3J = 7.2 Hz, CO–CH_2), 1.88 (t, 2H, ^3J = 7.3 Hz, CO–CH_2), 1.46–1.32 (m, 4H, (CH_2)$_2$), 1.20–1.06 (m, 4H, (CH_2)$_2$); ^{13}C NMR (75.5 MHz, DMSO-d_6) δ = 172.01, 171.84, 169.00 (*C*O), 152.89, 142.41, 136.45, 129.32, 128.57, 123.13, 111.71 105.18 (Ar-*C*), 53.03, 51.51 (COO*C*H_3, NH–*C*H–CO), 36.34 (CH–*C*H_2–Ar), 34.80, 32.04 (CO–*C*H_2), 28.14, 27.99, 24.79 ((CH_2)$_4$).

4.2.28. (*S*)-3-(4-Furan-2-yl-phenyl)-2-(8-hydroxycarbamoyl-octanoylamino)-propionic acid methyl ester (4g). Compound **4g** was synthesized by method **F** from **11g** (150 mg, 0.22 mmol), 1.5 ml dichloromethane, TFA and TES; yield 59 mg (62%) grey powder; melting point: 135 °C; MS (ESI neg.) *m*/*z* = 429 $[M-H]^-$; IR (ATR) *v* (cm^{-1}) = 1751 ($COOCH_3$), 1639 (CO–NH, CO–NH–OH); ^1H NMR (300 MHz, DMSO-d_6) δ = 10.28 (s, 1H, *H*O–NH–CO), 8.62 (s, 1H, HO–N*H*–CO), 8.23 (d, 1H, ^3J = 8.1 Hz, N*H*–CH–CO), 7.71–7.70 (m, 1H, 5″-*H*), 7.61–7.58 (m, 2H, 3′/5′-*H*), 7.26–7.24 (m, 2H, 2′/6′-*H*), 6.89–6.88 (m, 1H, 3″-*H*), 6.56 (dd, 1H, ^3J = 3.3 Hz, ^3J = 1.8 Hz, 4″-*H*), 4.49 (ddd, 1H, ^3J = 9.7 Hz, ^3J = 8.1 Hz, ^3J = 5.4 Hz, NH–C*H*–CO), 3.60 (s, 3H, $COOCH_3$), 3.04 (dd, 1H, ^2J = 13.8 Hz, ^3J = 5.4 Hz, CH–CH_2–Ar), 2.87 (dd, 1H, ^2J = 13.8 Hz, ^3J = 9.7 Hz, CH–CH_2–Ar), 2.03 (t, 2H, ^3J = 7.2 Hz, CO–CH_2), 1.89 (t, 2H, ^3J = 7.4 Hz, CO–CH_2), 1.46–1.32 (m, 4H, (CH_2)$_2$), 1.20–1.03 (m, 6H, (CH_2)$_2$); ^{13}C NMR (75.5 MHz, DMSO-d_6) δ = 172.22, 172.11, 169.08 (*C*O), 152.96, 142.63, 136.58, 129.52, 128.67, 123.23, 111.94, 105.41 (Ar-*C*), 53.16, 51.77 (COO*C*H_3, NH–*C*H–CO), 36.40 (CH–*C*H_2–Ar), 34.93, 32.20 (CO–*C*H_2), 28.45, 28.42, 28.29, 25.07, 25.05 ((CH_2)$_5$).

4.2.29. (*S*)-3-(4-Furan-3-yl-phenyl)-2-(7-hydroxycarbamoyl-heptanoylamino)-propionic acid methyl ester (4h). Compound **4h** was synthesized by method **F** from **11h** (310 mg, 0.47 mmol), 3.1 ml dichloromethane, TFA and TES; yield 106 mg (54%) grey powder; melting point: 141 °C; MS (ESI pos.) *m*/*z* = 439 $[M+Na]^+$; IR (ATR) *v* (cm^{-1}) = 1738 ($COOCH_3$), 1623 (CO–NH, CO–NH–OH); ^1H NMR (300 MHz, DMSO-d_6) δ = 10.31 (s, 1H, *H*O–NH–CO), 8.65 (s, 1H, HO–N*H*–CO), 8.26 (d, 1H, ^3J = 7.9 Hz, N*H*–CH–CO), 8.16 (dd, 1H, ^4J = 1.7 Hz, ^4J = 0.9 Hz, 2″-*H*), 7.73 (pt, 1H, ^2J = 1.7 Hz, ^3J = 1.7 Hz, 5″-*H*), 7.53–7.51 (m, 2H, 3′/5′-*H*), 7.23–7.21 (m, 2H, 2′/6′-*H*), 6.95 (dd, 1H, ^3J = 1.7 Hz, ^4J = 0.9 Hz, 4″-*H*), 4.48 (ddd, 1H, ^3J = 9.7 Hz, ^3J = 7.9 Hz, ^3J = 5.3 Hz, NH–C*H*–CO), 3.61 (s, 3H, $COOCH_3$), 3.03 (dd, 1H, ^2J = 13.8 Hz, ^3J = 5.3 Hz, CH–CH_2–Ar), 2.87 (dd, 1H, ^2J = 13.8 Hz, ^3J = 9.7 Hz, CH–CH_2–Ar), 2.04 (t, 2H, ^3J = 7.3 Hz, CO–CH_2), 1.90 (t, 2H, ^3J = 7.4 Hz, CO–CH_2), 1.46–1.35 (m, 4H, (CH_2)$_2$), 1.20–1.08 (m, 4H, (CH_2)$_2$); ^{13}C NMR (75.5 MHz, DMSO-d_6) δ = 172.23, 172.14, 169.05 (*C*O), 144.14, 139.04, 135.94, 130.15, 129.44, 125.55, 125.31, 108.58 (Ar-*C*), 53.32, 51.75 (COO*C*H_3, NH–*C*H–CO), 36.34 (CH–*C*H_2–Ar), 34.91, 32.19 (CO–*C*H_2), 28.30, 28.15, 25.00, 24.95 ((CH_2)$_4$).

4.2.30. (*S*)-3-(4-Furan-3-yl-phenyl)-2-(8-hydroxycarbamoyl-octanoylamino)-propionic acid methyl ester (4i). Compound **4i** was synthesized by method **G** from **11i** (300 mg, 0.45 mmol), 8.9 ml dichloromethane, 1 μl TMSTF and 85 μl TES; yield: 147 mg (76%) grey powder; melting point: 138 °C; MS (ESI pos.) *m*/*z* = 431 $[M+H]^+$; IR (ATR) *v* (cm^{-1}) = 1733 ($COOCH_3$), 1646, 1623 (CO–NH, CO–NH–OH); ^1H NMR (300 MHz, DMSO-d_6) δ = 10.28 (s, 1H, *H*O–NH–CO), 8.62 (s, 1H, HO–N*H*–CO), 8.22 (d, 1H, ^3J = 8.0 Hz, N*H*–CH–CO), 8.12 (m, 2″-*H*), 7.70 (pt, 1H, ^2J = 1.7 Hz, ^3J = 1.7 Hz, 5″-*H*), 7.51–7.49 (m, 2H, 3′/5′-*H*), 7.22–7.19 (m, 2H, 2′/6′-*H*), 6.92 (dd, 1H, ^3J = 1.7 Hz, ^4J = 0.8 Hz, 4″-*H*), 4.48 (ddd, 1H, ^3J = 9.4 Hz, ^3J = 8.0 Hz, ^3J = 5.3 Hz, NH–C*H*–CO), 3.60 (s, 3H, $COOCH_3$), 3.02 (dd, 1H, ^2J = 13.8 Hz, ^3J = 5.3 Hz, CH–CH_2–Ar), 2.86 (dd, 1H, ^2J = 13.8 Hz, ^3J = 9.4 Hz, CH–CH_2–Ar), 2.03 (t, 2H, ^3J = 7.2 Hz, CO–CH_2), 1.89 (t, 2H, ^3J = 7.3 Hz, CO–CH_2), 1.46–1.33 (m, 4H, (CH_2)$_2$), 1.19–1.04 (m, 6H, (CH_2)$_3$); ^{13}C NMR (75.5 MHz, DMSO-d_6) δ = 172.25, 172.15, 169.09 (*C*O), 144.15, 139.03, 135.93, 130.14, 129.44, 125.55, 125.30, 108.57 (Ar-*C*), 53.28, 51.76 (COO*C*H_3, NH–*C*H–CO), 36.34 (CH–*C*H_2–Ar), 34.93, 32.20 (CO–*C*H_2), 28.44, 28.42, 28.30, 25.05 ((CH_2)$_5$).

4.2.31. (*S*)-2-(7-Hydroxycarbamoyl-heptanoylamino)-3-[1,1′:4′,1″]terphenyl-4-yl-propionic acid methyl ester (4j).

Compound **4j** was synthesized by method **F** from **11j** (280 mg, 0.38 mmol), 2.8 ml dichloromethane, TFA and TES; yield 107 mg (56%) grey powder; melting point: 176 °C; MS (ESI pos.) *m/z* = 525 $[M+Na]^+$; IR (ATR) *v* (cm^{-1}) = 1737 ($COOCH_3$), 1646 (CO–NH, CO–NH–OH); ^1H NMR (300 MHz, DMSO-d_6) δ = 10.28 (s, 1H, *H*O–NH–CO), 8.61 (s, 1H, HO–N*H*–CO), 8.27 (d, 1H, ^3J = 8.0 Hz, N*H*–CH–CO), 7.73–7.29 (m, 13H, Ar-*H*), 4.49 (ddd, 1H, ^3J = 9.5 Hz, ^3J = 8.0 Hz, ^3J = 5.3 Hz, NH–C*H*–CO), 3.61 (s, 3H, $COOCH_3$), 3.07 (dd, 1H, ^2J = 13.9 Hz, ^3J = 5.3 Hz, CH–CH_2–Ar), 2.92 (dd, 1H, ^2J = 13.9 Hz, ^3J = 9.5 Hz, CH–CH_2–Ar), 2.05 (t, 2H, ^3J = 7.4 Hz, CO–CH_2), 1.88 (t, 2H, ^3J = 7.4 Hz, CO–CH_2), 1.46–1.35 (m, 4H, (CH_2)$_2$), 1.19–1.09 (m, 4H, (CH_2)$_2$); ^{13}C NMR (75.5 MHz, DMSO-d_6) δ = 172.29, 172.16, 169.06 (*C*O), 139.57, 138.95, 138.78, 137.69, 136.74, 129.66, 128.93, 127.45, 127.12, 126.93, 126.50, 126.27 (Ar-*C*), 53.29, 51.79 ($COOCH_3$, NH–*C*H–CO), 36.26 (CH–*C*H_2–Ar), 34.93, 32.20 (CO–*C*H_2), 28.31, 28.16, 25.00, 24.96 ((CH_2)$_4$).

4.2.32. (*S*)-2-(8-Hydroxycarbamoyl-octanoylamino)-3-[1,1′:4′,1″]terphenyl-4-yl-propionic acid methyl ester (4k). Compound **4k** was synthesized by method **F** from **11k** (370 mg, 0.49 mmol), 3.7 ml dichloromethane, TFA and TES; yield 216 mg (85%) grey powder; melting point: 193 °C; MS (ESI pos.) *m/z* = 517 $[M+H]^+$; IR (ATR) *v* (cm^{-1}) = 1742 ($COOCH_3$), 1653, 1616 (CO–NH, CO–NH–OH); ^1H NMR (300 MHz, DMSO-d_6) δ = 10.28 (s, 1H, *H*O–NH–CO), 8.62 (s, 1H, HO–N*H*–CO), 8.26 (d, 1H, ^3J = 8.0 Hz, N*H*–CH–CO), 7.73–7.29 (m, 13H, Ar-*H*), 4.49 (ddd, 1H, ^3J = 9.6 Hz, ^3J = 8.0 Hz, ^3J = 5.2 Hz, NH–C*H*–CO), 3.61 (s, 3H, $COOCH_3$), 3.07 (dd, 1H, ^2J = 13.8 Hz, ^3J = 5.2 Hz, CH–CH_2–Ar), 2.91 (dd, 1H, ^2J = 13.8 Hz, ^3J = 9.6 Hz, CH–CH_2–Ar), 2.05 (t, 2H, ^3J = 7.2 Hz, CO–CH_2), 1.88 (t, 2H, ^3J = 7.4 Hz, CO–CH_2), 1.46–1.34 (m, 4H, (CH_2)$_2$), 1.20–1.08 (m, 6H, (CH_2)$_3$); ^{13}C NMR (75.5 MHz, DMSO-d_6) δ = 172.34, 172.18, 169.11 (*C*O), 139.59, 138.98, 138.80, 137.70, 136.75, 129.68, 128.95, 127.46, 127.13, 126.93, 126.52, 126.28 (Ar-*C*), 53.28, 51.81 ($COOCH_3$, NH–*C*H–CO), 36.28 (CH–*C*H_2–Ar), 34.97, 32.22 (CO–*C*H_2), 28.46, 28.45, 28.32, 25.09, 25.08 ((CH_2)$_5$).

4.2.33. (*S*)-2-(7-Hydroxycarbamoyl-heptanoylamino)-3-(4-naphthalen-2-yl-phenyl)-propionic acid methyl ester (4l). Compound **4l** was synthesized by method **F** from **11l** (230 mg, 0.32 mmol), 2.3 ml dichloromethane, TFA and TES; yield 107 mg (70%) grey powder; melting point: 130 °C; MS (ESI pos.) *m/z* = 477 $[M+H]^+$, 499 $[M+Na]^+$; IR (ATR) *v* (cm^{-1}) = 1742 ($COOCH_3$), 1653, 1616 (CO–NH, CO–NH–OH); ^1H NMR (300 MHz, DMSO-d_6) δ = 10.28 (s, 1H, *H*O–NH–CO), 8.61 (s, 1H, HO–N*H*–CO), 8.28 (d, 1H, ^3J = 8.0 Hz, N*H*–CH–CO), 8.18 (br s, 1H, 1″-*H*), 7.99–7.96 (m, 2H, 5″/8″-*H*), 7.92–7.89 (m, 1H, 4″-H), 7.83–7.80 (m, 1H, 3″-H), 7.74–7.71 (m, 2H, 3′/5′-*H*), 7.55–7.46 (m, 2H, 6″/7″-*H*), 7.35–7.32 (m, 2H, 2′/6′-*H*), 4.54 (ddd, 1H, ^3J = 9.5 Hz, ^3J = 8.0 Hz, ^3J = 5.3 Hz, NH–C*H*–CO), 3.62 (s, 3H, $COOCH_3$), 3.09 (dd, 1H, ^2J = 13.8 Hz, ^3J = 5.3 Hz, CH–CH_2–Ar), 2.93 (dd, 1H, ^2J = 13.8 Hz, ^3J = 9.5 Hz, CH–CH_2–Ar), 2.05 (t, 2H, ^3J = 7.3 Hz, CO–CH_2), 1.87 (t, 2H, ^3J = 7.3 Hz, CO–CH_2), 1.46–1.35 (m, 4H, (CH_2)$_2$), 1.19–1.09 (m, 4H, (CH_2)$_2$); ^{13}C NMR (75.5 MHz, DMSO-d_6) δ = 172.30, 172.16, 169.05 (*C*O), 138.07, 137.13, 136.78, 133.30, 132.13, 129.69, 128.38, 128.11, 127.41, 126.68, 126.32, 125.98, 124.92, 124.90 (Ar-*C*), 53.33, 51.80 ($COOCH_3$, NH–*C*H–CO), 36.28 (CH–*C*H_2–Ar), 34.92, 32.20 (CO–*C*H_2), 28.30, 28.16, 25.00, 24.96 ((CH_2)$_4$).

4.2.34. (*S*)-2-(8-Hydroxycarbamoyl-octanoylamino)-3-(4-naphthalen-2-yl-phenyl)-propionic acid methyl ester (4m). Compound **4m** was synthesized by method **F** from **11m** (300 mg, 0.41 mmol), 3.0 ml dichloromethane, TFA and TES; yield 158 mg (79%) grey powder; melting point: 160 °C; MS (ESI pos.) *m/z* = 491 $[M+H]^+$, 513 $[M+Na]^+$; IR (ATR) *v* (cm^{-1}) = 1744 ($COOCH_3$), 1652, 1615 (CO–NH, CO–NH–OH); ^1H NMR (300 MHz, DMSO-d_6) δ = 10.28 (s, 1H, *H*O–NH–CO), 8.62 (s, 1H, HO–N*H*–CO), 8.28 (d, 1H, ^3J = 8.0 Hz, N*H*–CH–CO), 8.19 (br s, 1H, 1″-*H*), 8.00–7.96 (m, 2H, 5″/8″-*H*), 7.93–7.90 (m, 1H, 4″-H), 7.84–7.81 (m, 1H, 3″-H), 7.74–7.71 (m, 2H, 3′/5′-*H*), 7.56–7.47 (m, 2H, 6″/7″-*H*), 7.36–7.33 (m, 2H, 2′/6′-*H*), 4.54 (ddd, 1H, ^3J = 9.5 Hz, ^3J = 8.0 Hz, ^3J = 5.4 Hz, NH–C*H*–CO), 3.63 (s, 3H, $COOCH_3$), 3.10 (dd, 1H, ^2J = 13.8 Hz, ^3J = 5.4 Hz, CH–CH_2–Ar), 2.82 (dd, 1H, ^2J = 13.8 Hz, ^3J = 9.5 Hz, CH–CH_2–Ar), 2.06 (t, 2H, ^3J = 7.3 Hz, CO–CH_2), 1.88 (t, 2H, ^3J = 7.3 Hz, CO–CH_2), 1.46–1.36 (m, 4H, (CH_2)$_2$), 1.20–1.10 (m, 6H, (CH_2)$_3$); ^{13}C NMR (75.5 MHz, DMSO-d_6) δ = 172.28, 172.14, 169.03 (*C*O), 138.04, 137.12, 136.76, 133.28, 132.12, 129.68, 128.36, 128.08, 127.40, 126.65, 126.31, 125.96, 124.89 (Ar-*C*), 53.29, 51.78 ($COOCH_3$, NH–*C*H–CO), 36.28 (CH–*C*H_2–Ar), 34.93, 32.17 (CO–*C*H_2), 28.42, 28.40, 28.30, 25.05, 25.03 ((CH_2)$_5$).

4.2.35. (*S*)-3-(4-Bromo-phenyl)-2-(7-hydroxycarbamoyl-heptanoylamino)-propionic acid methyl ester (4n). Compound **4n** was synthesized by method **F** from **10a** (100 mg, 0.15 mmol), 1.0 ml dichloromethane, TFA and TES; yield 33 mg (51%) grey powder; melting point: 150 °C; (ESI pos.) *m/z* = 451/453 $[M+Na]^+$; IR (ATR) *v* (cm^{-1}) = 1736 ($COOCH_3$), 1620 (CO–NH, CO–NH–OH); ^1H NMR (300 MHz, DMSO-d_6) δ = 10.21 (s, 1H, *H*O–NH–CO), 8.49 (s, 1H, HO–N*H*–CO), 8.10 (d, 1H, ^3J = 8.1 Hz, N*H*–CH–CO), 7.47–7.42 (m, 2H, 3′/5′-*H*), 7.18–7.13 (m, 2H, 2′/6′-*H*), 4.49 (ddd, 1H, ^3J = 9.4 Hz, ^3J = 8.1 Hz, ^3J = 5.4 Hz, NH–C*H*–CO), 3.60 (s, 3H, $COOCH_3$), 3.01 (dd, 1H, ^2J = 13.8 Hz, ^3J = 5.4 Hz, CH–CH_2–Ar), 2.85 (dd, 1H, ^2J = 13.8 Hz, ^3J = 9.4 Hz, CH–CH_2–Ar), 2.03 (t, 2H, ^3J = 7.3 Hz, CO–CH_2), 1.93 (t, 2H, ^3J = 6.8 Hz, CO–CH_2), 1.50–1.34 (m, 4H, (CH_2)$_2$), 1.24–1.07 (m, 4H, (CH_2)$_2$); ^{13}C NMR (75.5 MHz, DMSO-d_6) δ = 172.00, 171.68, 168.95 (*C*O), 136.62, 131.07, 130.78, 119.46 (Ar-*C*), 52.79, 51.54 ($COOCH_3$, NH–*C*H–CO), 35.88 (CH–*C*H_2–Ar), 34.78, 32.07 (CO–*C*H_2), 28.14, 27.96, 24.76 ((CH_2)$_4$).

4.2.36. (*S*)-3-(4-Bromo-phenyl)-2-(8-hydroxycarbamoyl-octanoylamino)-propionic acid methyl ester (4o). Compound **4o** was synthesized by method **F** from **10b** (200 mg, 0.29 mmol), 2.0 ml dichloromethane, TFA and TES; yield 115 mg (89%) grey powder; melting point: 140 °C; (ESI pos.) *m/z* = 465/467 $[M+Na]^+$; IR (ATR) *v* (cm^{-1}) = 1736 ($COOCH_3$), 1619 (CO–NH, CO–NH–

OH); ^{1}H NMR (300 MHz, DMSO-d_6) δ = 10.29 (s, 1H, *H*O–NH–CO), 8.61 (s, 1H, HO–N*H*–CO), 8.21 (d, 1H, ^3J = 8.0 Hz, N*H*–CH–CO), 7.46–7.43 (m, 2H, 3′/5′-*H*), 7.18–7.15 (m, 2H, 2′/6′-*H*), 4.47 (ddd, 1H, ^3J = 9.8 Hz, ^3J = 8.0 Hz, ^3J = 5.3 Hz, NH–C*H*–CO), 3.59 (s, 3H, COOCH_3), 3.01 (dd, 1H, ^2J = 13.9 Hz, ^3J = 5.3 Hz, CH–CH_2–Ar), 2.82 (dd, 1H, ^2J = 13.9 Hz, ^3J = 9.8 Hz, CH–CH_2–Ar), 2.01 (t, 2H, ^3J = 7.2 Hz, CO–CH_2), 1.92 (t, 2H, ^3J = 7.4 Hz, CO–CH_2), 1.47–1.31 (m, 4H, (CH_2)$_2$), 1.19–1.02 (m, 6H, (CH_2)$_3$); ^{13}C NMR (75.5 MHz, DMSO-d_6) δ = 172.70, 172.45, 169.57 (*C*O), 137.27, 131.79, 131.47, 120.15 (Ar-*C*), 53.44, 52.31 (COO*C*H$_3$, NH–*C*H–CO), 36.45 (CH–*C*H$_2$–Ar), 35.43, 32.73 (CO–*C*H$_2$), 28.94, 28.76, 25.58, 25.54 ((*C*H$_2$)$_5$).

4.3. Assays

4.3.1. Assays with rat liver extract. Enzyme inhibition of the new inhibitors on HDACs was determined using standard methods that have previously been reported. Rat liver HDAC was purified by ammonium sulfate precipitation and chromatography on Q-Sepharose as described. To get a first idea of the potential of the new compounds we used this partially purified extract with a fluorescent substrate (MAL)[35] that was shown to be unselective[21] for different subtypes. In a second test series we used the same extract with subtype selective substrates previously discovered in our group[21] in order to discover compounds showing subtype selectivity. For HDAC1 prediction *Z*-(propionyl)Lys-AMC and for HDAC6 prediction Boc(Ac)Lys-(F_3-AMC) were used.

Stock solutions of the inhibitors **4a**–**o** were prepared at 12 mM in DMSO and further diluted with enzyme buffer [1.4 mM NaH_2PO_4, 18.6 mM Na_2HPO_4, pH 7.9, 0.25 mM EDTA, 10 mM NaCl, 10% (v/v) glycerol and 10 mM 2-mercaptoethanol] to the desired concentration. Stock solutions of the substrates were prepared at 12.6 mM in DMSO and also further diluted with enzyme buffer to a concentration of 126 μM and used for the assay. Fifty microliters of rat liver extract was then incubated with 5 μl of the inhibitor dilution and 5 μl of the substrate dilution at 37 °C. Incubation times were 90 min for the unselective substrates and 180 min for the selective substrates, respectively. The reaction was stopped by adding 190 μl of freshly prepared stop solution (TSA 3.3 μM, borate buffer, pH 9.5, and naphthalene-2,3-dicarboxaldehyde (NDA, 16 mM in methanol) in a ratio of 5:190:5). The samples were measured at an excitation wavelength of 330 nm and an emission wavelength of 390 nm except for HDAC6-selective substrate (excitation 340 nm, emission 430 nm). For compound **4m** we had to use a different version of the assay due to interferences with the test system by the inhibitor. After incubation of the enzyme with the inhibitor instead of NDA trypsin was used in order to develop the reaction according to the literature.[36–38]

4.3.2. Immunoprecipitated FLAG-tagged HDAC1 and HDAC6. To verify the data generated with the subtype selective substrates in the rat liver extract test system, we isolated FLAG-tagged HDAC1 and HDAC6 from 293T cell lines overexpressing either HDAC1 or HDAC6 with M2-agarose beads (Sigma) as previously described. We used the purified subtypes to determine the inhibitory potential using an unselective substrate (called ZMAL)[20] that was shown to be suitable for this test system.

293T cell lines overexpressing FLAG-tagged HDAC1 and HDAC6 were cultured and lysed. M2 agarose was used at 25 μl/ml cell lysate. The immunoprecipitated enzymes were washed in enzyme buffer, diluted (1:10) and used as an enzyme source. Fifty microliters of beads suspension was incubated with 5 μl of the inhibitor dilution and 5 μl of the substrate dilution at 37 °C for 180 min. The reaction was stopped by adding 190 μl of freshly prepared stop solution (3.3 μM TSA, borate buffer, pH 9.5, and naphthalene-2,3-dicarboxaldehyde (16 mM in methanol) in a ratio of 5:180:5). The samples were measured at an excitation wavelength of 330 nm and an emission wavelength of 390 nm.

4.3.3. Determination of IC_{50}-values. The amount of remaining substrate in the samples was calculated relative to two standards equivalent to 0% and 100% enzyme inhibition. For 100% inhibition we used 50 μl of enzyme source, 5 μl of a 3.3 μM TSA dilution and 5 μl of the substrate dilution. For 0% inhibition we used 50 μl of enzyme source, 5 μl of enzyme buffer and 5 μl of the substrate dilution. The IC_{50}-values were determined by measuring the enzyme inhibition of a dilution series of the particular inhibitor in relation to the standards and following evaluation with the GraphPadPrism software.

4.3.4. Cell proliferation. For cell proliferation assays, cells were seeded at 5000 per well in 80 μl of growing medium in 96-well tissue culture plates. At 24 h after seeding, diluted compounds or DMSO vehicle control was added to each well to a total volume of 100 μl (three replicates per concentration) and incubated for 48 h at 37 °C. Growth inhibition was determined using One-Aqueous Proliferation Assay (MTS, Promega, Madison, WI) according to manufacturer's instructions, and the absorbance measured at 490 nm on a microplate reader. The 50% growth inhibition (GI_{50}) was calculated as the compound concentration required to reduce cell number by 50% compared with control using GraphPad Prism 4.0.

4.3.5. Western blot analysis. HCT116 human colon carcinoma cells were grown in Dulbecco's modified Eagle's medium (DMEM; Mediatech, Herndon, VA) supplemented with 10% foetal bovine serum (FBS; Gemini Bio-products, Woodland, CA), 1% penicillin–streptomycin and 2 mM L-glutamine (Gibco Invitrogen Corporation). The cells were treated with different concentrations of the inhibitors **4d**, **4e**, **4n** and TSA as a control for 6 h. Cells were lysed in 50 mM Tris–HCl (pH 7.5), 0.5 mM EDTA, 150 mM NaCl, 0.5% NP-40 and 1× complete protease inhibitors (Roche, Penzberg, Germany), and protein concentration was determined with the D_C Protein Assay (Bio-Rad). Protein samples were electrophoresed on 10% and 15% SDS–polyacrylamide gels and transferred to a nitrocellulose membrane

(Bio-Rad). Membranes were blocked with 5% non-fat dried milk in TBS–Tween (10 mM Tris–HCl (pH 7.5), 150 mM NaCl and 0.1% Tween 20) and probed with anti-acetylated α-tubulin (6-11B-1; Sigma) or anti-α-tubulin (B-5-1-2; Sigma) at 1:2000, anti-acetylated histone H3 (06-599; Upstate) and anti-acetylated histone H4 (06-866; Upstate).

4.4. X-ray crystallography

4.4.1. Crystallization and data collection. Highly purified HDAH was obtained as described before.[18] Crystals were obtained at 20 °C after 3–4 days using the sitting drop vapour diffusion method in Chryschem plates (Hampton Research, Riverside, USA) sealed with clear tape by mixing equal volumes of FB188 HDAH with reservoir solution (inhibitor crystals: 600 mM NaCl, 200 mM Na-Cacodylate, pH 6.5). The size of the crystals was increased by seeding crystals into a fresh drop in the presence of 0.2 mM zinc-acetate and a fivefold excess of the inhibitor ST-17. 20–25% glycerol added to the reservoir solution served as cryoprotectant. The crystals are primitive monoclinic. X-ray data were collected from cryo-cooled crystals at beamlines X13 ($\lambda = 0.8015$ Å) at the EMBL Outstation Hamburg. The data were processed with HKL2000 (HKL Research, Charlottesville, USA). The unit cell parameters are shown in Table 3. Systematic absences along the b axis indicated that the monoclinic space group was $P2_1$. The Matthews coefficient was 2.5 Å^3/Da suggesting for four molecules in the asymmetric unit corresponding to a solvent content of 50.8%, respectively.

4.4.2. Structure determination and refinement. The structure of the HDAH in complex with **4n** was determined by molecular replacement and refined using REFMAC5[39] with 5% of the reflections omitted in the refinement for the calculation of R_{free}.[40] Water molecules were added automatically with the ARP/wARP function[41] in REFMAC5 and afterwards examined manually for reasonable hydrogen bonding. The final models consist of either residues 7–374 for one molecule (A) or 8–375 for the other three molecules in the asymmetric unit. The refinement statistics are summarized in Table 1. The restraints for **4n** used in the refinement were created with PRODRG.[42] The quality of the model was checked using PROCHECK[43] and was found to be good. 90% of the residues are located in the most favourable region of the Ramachandran plot. Superpositions enabling comparison of the different structures are performed in LSQMAN[44] using the brute-force option. All figures are made in PYMOL (The PyMOL Molecular Graphics System (2002), DeLano Scientific, San Carlos, USA).

4.5. Molecular modelling

All calculations were performed on a Pentium 1.8 GHz Linux cluster. The molecular structures of the inhibitors were generated using the MOE modelling package (Chemical Computing Group, Montreal, Canada). The structures were energy minimized using the MMFF94s force field and the conjugate gradient method, until the default derivative convergence criterion of 0.01 kcal/(mol Å) was met.

4.5.1. Generation of homology models for HDAC1 and HDAC6. The X-ray structures of HDAC8 and HDLP were used as templates for the generation of a homology model for HDAC1, whereas HDAC7 was used as template for modelling both catalytic domains (CD) of HDAC6. HDAC-6 is unique among deacetylases in having two HDAC domains (HDAC6 CD I and HDCA6 CD II) sharing 41% and 49 % sequence identity with HDAC7, respectively. Sequences were obtained from the Uniprot database.[45] Multiple sequence alignment of human HDAC1, HDAC8, HDAC7, HDAC6 CD I and CD II, bacterial HDLP and HDAH was carried out using CLUSTALW[46] using the BLOSUM matrices for scoring the alignments. The sequence identity between the different HDACs and the resulting sequence alignment are shown in Fig. F and Table A in the Supporting Information. Coordinates of the template structures (HDAC8: 1T64.pdb; HDAC7: 2PQO.pdb; HDLP: 1C3R.pdb) were retrieved from the Protein Database.[32] Homology models for human HDAC1 and HDAC6 were generated on the basis of the best-scored alignment (Fig. E, Supplementary material) and using the COMPOSER module as part of the Sybyl 7.2 program.[47] The loop region Gln26-Pro32 in HDAC1 was modelled on the basis of the HDLP structure, due to higher sequence identity (for details, see the sequence alignment in the Supporting Information). The visualization of the molecular surface was carried out using the MOLCAD module within Sybyl 7.2.

4.5.2. Molecular dynamics (MD) simulations. All models were refined by minimization procedures and MD simulation approaches using the GROMACS software.[48] A solvent box with dimensions $5.6 \times 5.4 \times 6.0$ nm was generated in order to perform simulations in an aqueous environment. The protonation state of each amino acid residue was adjusted according to the pK_a values in a medium of pH 7.4. Protonation states of histidines were selected manually by considering the protein environment and potential hydrogen bond partners. Water molecules were represented with the simple point charge (SPC) model.[49] Na^+ and Cl^- counter-ions were added by replacing water molecules to ensure the overall neutrality of the simulated system. The models were minimized using 8000 iterations of steepest descent within the GROMOS96 force field.[47] Molecular dynamics (MD) simulations with periodic boundary conditions were performed at 310 K. The Particle-mesh Ewald (PME) method was used for accurate determination of long-range electrostatic interactions.[50,51] van der Waals interactions were considered applying a cut-off of 0.9 nm. The timestep for the simulations was set to 1 fs. To keep the system at constant temperature a Berendsen thermostat was applied using a coupling time of 0.1 ps.[52] Constant pressure was maintained by coupling to an external bath with a reference value of 105 Pa, with a coupling time of 0.5 ps and an isothermal compressibility of $4.5 \times 10–10$ Pa^{-1}. For the homology models 1 ns equilibration run with decreasing constraints on backbone atoms (1000–250 kJ mol^{-1}) were employed.

Free MD simulations were carried out for 3.15 ns. Bonds between heavy atoms and corresponding hydrogen atoms were constrained to their equilibrium bond lengths using the LINCS algorithm.[53] The RMSD of the backbone atoms was stabilized after 2 ns. Thus, the average protein structure from a time frame of 2–3.5 ns was calculated, and further energy-minimization steps with the steepest descent method were performed to create the final HDAC protein structures used in the study. Heavy atom RMSD values between the final protein structure and the starting structure of the MD simulation were calculated to ensure that no large-scale structural arrangements have taken place during the MD simulation. The stereochemical quality of the resulting models was evaluated using PROCHECK and ProSa and compared with the X-ray structures.[43,54]

4.5.3. Docking study. Docking of the co-crystallized ligands, as well as the tested inhibitors, was carried out using the HDAH X-ray structure as well as the HDAC1 and HDCAC6 homology models. Program GOLD 3.0 was taken for the ligand docking. All torsion angles in each compound were allowed to rotate freely. For each molecule, 30 docking runs were carried out. The resulting solutions were clustered on the basis of the heavy atom RMSD values (1 Å). We tested several docking setups in order to reproduce the experimentally derived complexes of HDAC inhibitors. The best agreement between the available X-ray structures and docking poses could be derived by applying the ChemScore scoring function within GOLD. A hydrogen bond between the active site histidines (His143 in HDAH, His141 in HDAC1, His216 in HDAC6 CD I, His611 in HDAC6 CD II) was used as docking constraint. This docking setup resulted in good reproduction (RMDS below 2.5 Å) of the experimentally derived structures of SAHA, CypY and compound **4n** which were co-crystallized with HDAH (for details, see Figs. A–D, Supporting Information). The top-ranked poses for each ligand were selected and viewed graphically within the MOE program.

Acknowledgments

S. Schäfer and M. Jung thank the Hans and Gertie Fischer-Foundation for funding and Sanofi-Aventis for an [i]lab travel award. We thank the staff at the EMBL-outstation Hamburg, especially Matthew Groves for guidance during data collection at DESY beamline X13.

Supplementary data

Supplementary data associated with this article can be found, in the online version, at doi:10.1016/j.bmc.2007.10.092.

References and notes

1. Johnstone, R. W. *Nat. Rev. Drug Discov.* **2002**, *1*, 287.
2. Minucci, S.; Pelicci, P. G. *Nat. Rev. Cancer* **2006**, *6*, 38.
3. Gray, S. G.; Ekstrom, T. J. *Exp. Cell Res.* **2001**, *262*, 75.
4. Schäfer, S.; Jung, M. *Arch. Pharm. Chem. Life Sci.* **2005**, *338*, 347.
5. Biel, M.; Wascholowski, V.; Giannis, A. *Angew. Chem., Int. Ed. Engl.* **2005**, *44*, 3186.
6. Miller, T. A.; Witter, D. J.; Belvedere, S. *J. Med. Chem.* **2003**, *46*, 5097.
7. Wittich, S.; Scherf, H.; Xie, C.; Brosch, G.; Loidl, P.; Gerhauser, C.; Jung, M. *J. Med. Chem.* **2002**, *45*, 3296.
8. Wittich, S.; Scherf, H.; Xie, C.; Heltweg, B.; Dequiedt, F.; Verdin, E.; Gerhauser, C.; Jung, M. *Anticancer Drugs* **2005**, *16*, 635.
9. Furumai, R.; Matsuyama, A.; Kobashi, N.; Lee, K. H.; Nishiyama, M.; Nakajima, H.; Tanaka, A.; Komatsu, Y.; Nishino, N.; Yoshida, M.; Horinouchi, S. *Cancer Res.* **2002**, *62*, 4916.
10. Furumai, R.; Komatsu, Y.; Nishino, N.; Khochbin, S.; Yoshida, M.; Horinouchi, S. *Proc. Natl. Acad. Sci. U.S.A.* **2001**, *98*, 87.
11. Mai, A.; Massa, S.; Ragno, R.; Esposito, M.; Sbardella, G.; Nocca, G.; Scatena, R.; Jesacher, F.; Loidl, P.; Brosch, G. *J. Med. Chem.* **2002**, *45*, 1778.
12. Park, J. H.; Jung, Y.; Kim, T. Y.; Kim, S. G.; Jong, H. S.; Lee, J. W.; Kim, D. K.; Lee, J. S.; Kim, N. K.; Bang, Y. J. *Clin. Cancer Res.* **2004**, *10*, 5271.
13. Hess-Stumpp, H.; Bracker, T. U.; Henderson, D.; Politz, O. *Int. J. Biochem. Cell Biol.* **2007**.
14. Suzuki, T.; Kouketsu, A.; Itoh, Y.; Hisakawa, S.; Maeda, S.; Yoshida, M.; Nakagawa, H.; Miyata, N. *J. Med. Chem.* **2006**, *49*, 4809.
15. Mai, A.; Massa, S.; Pezzi, R.; Simeoni, S.; Rotili, D.; Nebbioso, A.; Scognamiglio, A.; Altucci, L.; Loidl, P.; Brosch, G. *J. Med. Chem.* **2005**, *48*, 3344.
16. Haggarty, S. J.; Koeller, K. M.; Wong, J. C.; Grozinger, C. M.; Schreiber, S. L. *Proc. Natl. Acad. Sci. U.S.A.* **2003**, *100*, 4389.
17. Hildmann, C.; Wegener, D.; Riester, D.; Hempel, R.; Schober, A.; Merana, J.; Giurato, L.; Guccione, S.; Nielsen, T. K.; Ficner, R.; Schwienhorst, A. *J. Biotechnol.* **2006**, *124*, 258.
18. Nielsen, T. K.; Hildmann, C.; Dickmanns, A.; Schwienhorst, A.; Ficner, R. *J. Mol. Biol.* **2005**, *354*, 107.
19. Jung, M.; Brosch, G.; Kölle, D.; Scherf, H.; Gerhäuser, C.; Loidl, P. *J. Med. Chem.* **1999**, *42*, 4669.
20. Heltweg, B.; Dequiedt, F.; Verdin, E.; Jung, M. *Anal. Biochem.* **2003**, *319*, 42.
21. Heltweg, B.; Dequiedt, F.; Marshall, B. L.; Brauch, C.; Yoshida, M.; Nishino, N.; Verdin, E.; Jung, M. *J. Med. Chem.* **2004**, *47*, 5235.
22. Finnin, M. S.; Donigian, J. R.; Cohen, A.; Richon, V. M.; Rifkind, R. A.; Marks, P. A.; Breslow, R.; Pavletich, N. P. *Nature* **1999**, *401*, 188.
23. Somoza, J. R.; Skene, R. J.; Katz, B. A.; Mol, C.; Ho, J. D.; Jennings, A. J.; Luong, C.; Arvai, A.; Buggy, J. J.; Chi, E.; Tang, J.; Sang, B. C.; Verner, E.; Wynands, R.; Leahy, E. M.; Dougan, D. R.; Snell, G.; Navre, M.; Knuth, M. W.; Swanson, R. V.; McRee, D. E.; Tari, L. W. *Structure* **2004**, *12*, 1325.
24. Nielsen, T. K.; Hildmann, C.; Riester, D.; Wegener, D.; Schwienhorst, A.; Ficner, R. *Acta Crystallogr. Sect. F Struct. Biol. Cryst. Commun.* **2007**, *63*, 270.
25. Schuetz, A.; Min, J. R.; Allali-Hassani, A.; Loppnau, P.; Kwiatkowski, N. P.; Mazitschek, R.; Edwards, A. M.; Arrowsmith, C. H.; Vedadi, M.; Bochkarev, A.; Plotnikov, A. N. PDB 2NVR, in press.
26. Ragno, R.; Mai, A.; Massa, S.; Cerbara, I.; Valente, S.; Bottoni, P.; Scatena, R.; Jesacher, F.; Loidl, P.; Brosch, G. *J. Med. Chem.* **2004**, *47*, 1351.

27. Park, H.; Lee, S. *J. Comput. Aided Mol. Des.* **2004**, *18*, 375.
28. Wang, D. F.; Helquist, P.; Wiech, N. L.; Wiest, O. *J. Med. Chem.* **2005**, *48*, 6936.
29. Zhang, Y.; Gilquin, B.; Khochbin, S.; Matthias, P. *J. Biol. Chem.* **2006**, *281*, 2401.
30. Zou, H.; Wu, Y.; Navre, M.; Sang, B. C. *Biochem. Biophys. Res. Commun.* **2006**, *341*, 45.
31. GOLD 3.0; CCDC Cambridge, UK.
32. Berman, H. M.; Westbrook, J.; Feng, Z.; Gilliland, G.; Bhat, T. N.; Weissig, H.; Shindyalov, I. N.; Bourne, P. E. *Nucleic Acids Res.* **2000**, *28*, 235.
33. Vannini, A.; Volpari, C.; Filocamo, G.; Casavola, E. C.; Brunetti, M.; Renzoni, D.; Chakravarty, P.; Paolini, C.; De Francesco, R.; Gallinari, P.; Steinkuhler, C.; Di Marco, S. *Proc. Natl. Acad. Sci. U.S.A.* **2004**, *101*, 15064.
34. Hideshima, T.; Bradner, J. E.; Wong, J.; Chauhan, D.; Richardson, P.; Schreiber, S. L.; Anderson, K. C. *Proc. Natl. Acad. Sci. U.S.A.* **2005**, *102*, 8567.
35. Hoffmann, K.; Brosch, G.; Loidl, P.; Jung, M. *Nucleic Acids Res.* **1999**, *27*, 2057.
36. Wegener, D.; Wirsching, F.; Riester, D.; Schwienhorst, A. *Chem. Biol.* **2003**, *10*, 61.
37. Wegener, D.; Hildmann, C.; Riester, D.; Schwienhorst, A. *Anal. Biochem.* **2003**, *321*, 202.
38. Heltweg, B.; Trapp, J.; Jung, M. *Methods* **2005**, *36*, 332.
39. Murshudov, G. N.; Vagin, A. A.; Lebedev, A.; Wilson, K. S.; Dodson, E. J. *Acta Crystallogr. Sect. D* **1999**, *55*, 247.
40. Brunger, A. T. *Acta Crystallogr. Sect. D* **1993**, *49*, 24.
41. Perrakis, A.; Morris, R.; Lamzin, V. S. *Nat. Struct. Biol.* **1999**, *6*, 458.
42. Schuttelkopf, A. W.; van Aalten, D. M. *Acta Crystallogr. Sect. D* **2004**, *60*, 1355.
43. Laskowski, R. A.; MacArthur, M. W.; Moss, D. S.; Thornton, J. M. *J. Appl. Crystallogr.* **1993**, *26*, 283.
44. Kleywegt, G. J. *Acta Crystallogr. Sect. D* **1996**, *52*, 842.
45. Boeckmann, B.; Bairoch, A.; Apweiler, R.; Blatter, M. C.; Estreicher, A.; Gasteiger, E.; Martin, M. J.; Michoud, K.; O'Donovan, C.; Phan, I.; Pilbout, S.; Schneider, M. *Nucleic Acids Res.* **2003**, *31*, 365.
46. Thompson, J. D.; Higgins, D. G.; Gibson, T. J. *Nucleic Acids Res.* **1994**, *22*, 4673.
47. SYBYL 7.2; Tripos Inc.: St. Louis, MO, USA, 2005.
48. GROMACS 3.2.1 University of Groningen (The Netherlands).
49. Berendsen, H. J. C.; Postma, J. P. M.; van Gunsteren, W. F.; Hermans, J.; B., P.; Reidel: Dordrecht, NL, 1981; p 331.
50. Darden, T.; York, D.; Pedersen, L. G. *J. Comp. Phys.* **1993**, *98*, 10089.
51. Essmann, U.; Perera, L.; Berkowitz, M. L.; Darden, T.; Lee, H.; Pedersen, L. G. *J. Comp. Phys.* **1995**, *103*, 8577.
52. Berendsen, H. J. C.; Postma, J. P. M.; DiNola, A.; Haak, J. R. *J. Chem. Phys.* **1984**, *81*, 3684.
53. Hess, B.; Becker, H.; Berendsen, H. J. C.; Fraajie, J. G. E. M. *J. Comp. Phys.* **1997**, *18*, 1463.
54. Sippl, M. J. *Proteins* **1993**, *17*, 355.